

## 1,2,4-Triazol-3-yl-thiopropyl-tetrahydrobenzazepines: A Series of Potent and Selective Dopamine D<sub>3</sub> Receptor Antagonists

Fabrizio Micheli,<sup>\*,§</sup> Giorgio Bonanomi,<sup>§</sup> Frank E. Blaney,<sup>‡</sup> Simone Braggio,<sup>§</sup> Anna Maria Capelli,<sup>#</sup> Anna Checchia,<sup>§</sup> Ornella Curcuruto,<sup>#</sup> Federica Damiani,<sup>⊗</sup> Romano Di Fabio,<sup>§</sup> Daniele Donati,<sup>§</sup> Gabriella Gentile,<sup>§</sup> Andy Gribble,<sup>†</sup> Dieter Hamprecht,<sup>§</sup> Giovanna Tedesco,<sup>#</sup> Silvia Terreni,<sup>§</sup> Luca Tarsi,<sup>§</sup> Andrew Lightfoot,<sup>†</sup> Geoff Stemp,<sup>∇</sup> Gregor MacDonald,<sup>∇</sup> Alex Smith,<sup>∇</sup> Michela Pecoraro,<sup>‡</sup> Marcella Petrone,<sup>§</sup> Ornella Perini,<sup>#</sup> Jacqui Piner,<sup>||</sup> Tino Rossi,<sup>§</sup> Angela Worby,<sup>‡</sup> Maria Pilla,<sup>§</sup> Enzo Valerio,<sup>§</sup> Cristiana Griffante,<sup>§</sup> Manolo Mugnaini,<sup>§</sup> Martyn Wood,<sup>†</sup> Claire Scott,<sup>†</sup> Michela Andreoli,<sup>§</sup> Laurent Lacroix,<sup>†</sup> Adam Schwarz,<sup>§</sup> Alessandro Gozzi,<sup>§</sup> Angelo Bifone,<sup>§</sup> Charles R. Ashby, Jr.,<sup>⊗</sup> Jim J. Hagan,<sup>†</sup> and Christian Heidbreder<sup>\*,§</sup>

Psychiatry Centre of Excellence, Molecular Discovery Research, and Safety Assessment, GlaxoSmithKline Medicine Research Centre, Via Fleming 4, 37135 Verona, Italy, Psychiatry Centre of Excellence, Neurology Centre of Excellence, Molecular Discovery Research, and Safety Assessment, GlaxoSmithKline Medicine Research Centre, NFSP, Harlow, UK, and Department of Pharmaceutical Sciences, St. John's University, Jamaica, New York 11439

Received May 14, 2007

The discovery of new highly potent and selective dopamine D<sub>3</sub> receptor antagonists has recently permitted characterization of the role of the dopamine D<sub>3</sub> receptor in a wide range of preclinical animal models. A novel series of 1,2,4-triazol-3-yl-thiopropyl-tetrahydrobenzazepines demonstrating a high level of D<sub>3</sub> affinity and selectivity with an excellent pharmacokinetic profile is reported here. In particular, the pyrazolyl derivative **35** showed good oral bioavailability and brain penetration associated with high potency and selectivity *in vitro*. *In vivo* characterization of **35** confirmed that this compound blocks the expression of nicotine- and cocaine-conditioned place preference in the rat, prevents nicotine-triggered reinstatement of nicotine-seeking behavior in the rat, reduces oral operant alcohol self-administration in the mouse, increases extracellular levels of acetylcholine in the rat medial prefrontal cortex, and potentiates the amplitude of the relative cerebral blood volume response to *d*-amphetamine in a regionally specific manner in the rat brain.

### Introduction

Following the isolation and characterization of the cDNA for the dopamine D<sub>3</sub> receptor,<sup>1</sup> subsequent studies indicated that D<sub>3</sub> receptors, as well as D<sub>3</sub> receptor mRNA, are primarily localized in limbic regions of the rat<sup>2,3</sup> and human<sup>4–6</sup> brain. This finding led to the postulate that D<sub>3</sub> receptors may be involved in the pathophysiology of drug addiction and schizophrenia. Thus, the high binding affinity of the dopamine D<sub>3</sub> receptor to endogenous dopamine, its high expression in the mesolimbic system, and its up-regulation in the ventral striatum of schizophrenic patients that are off antipsychotics, as well as its up-regulation in the ventral striatum of cocaine overdose victims, and in rodents after cocaine self-administration or behavioral sensitization to cocaine- or nicotine-associated cues support the hypothesis that the dopamine D<sub>3</sub> receptor is an attractive new target for the pharmacotherapeutic management of drug addiction and schizophrenia (for reviews see refs 7–11). Recent studies have also shown that selective dopamine D<sub>3</sub> receptor antagonists are efficacious in animal models of

cocaine-, nicotine-, alcohol-, and heroin-seeking behaviors. Importantly, in contrast with dopamine D<sub>2</sub> receptor antagonists, selective antagonism at dopamine D<sub>3</sub> receptors does not elicit catalepsy, does not affect spontaneous or stimulant-induced locomotion, does not increase serum prolactin levels, and does not increase dopamine levels in the neostriatum.<sup>7</sup>

The main medicinal chemistry work reported in this manuscript is related to the modification of the cyclohexyl ethyl linker of previously reported GSK amide molecules<sup>9</sup> with a thio-triazolyl moiety and with a major exploration of the benzazepine scaffold. We herein describe the SAR analysis of a range of 1,2,4-triazol-3-yl-thiopropyl-tetrahydrobenzazepines, which has provided highly potent and selective dopamine D<sub>3</sub> receptor antagonists.

### Chemistry

During the past decade, part of GSK research in CNS drug discovery was aimed at the discovery of novel chemical entities able to selectively modulate the dopamine D<sub>3</sub> receptor. The successful result of this work led to the well characterized *trans*-*N*-[4-[2-(6-cyano-1,2,3,4-tetrahydroisoquinolin-2yl)ethyl]-cyclohexyl]-4-quinolinecarboxamide (SB-277011, **1**)<sup>12</sup> and *trans*-3-(2-(4-((3-(3-(5-methyl-1,2,4-oxadiazolyl))phenyl)carboxamido)cyclohexyl)ethyl)-7-methylsulfonyl-2,3,4,5-tetrahydro-1*H*-3-benzazepine (SB-414796, **2**)<sup>13</sup> (Figure 1).

While these molecules proved to be very useful for target validation, part of their overall developability profile, including

<sup>a</sup> Abbreviations: CPP, conditioned place preference; Ach, acetylcholine; hERG, human ether-a-go-go K<sup>+</sup> channel; NCE, novel chemical entity; PK, pharmacokinetic; P450, cytochrome P450; hCl<sub>i</sub>, human intrinsic clearance; MW, molecular weight; clogD, calculated logD; PSA, polar surface area; F%, bioavailability; B/B, brain/blood; Cl<sub>b</sub>, blood clearance; V<sub>d</sub>, distribution volume; SDM, site-directed mutagenesis; rCBV, relative cerebral blood volume; FLIPR, fluorescent imaging plate reader; GPCR, G-protein coupled receptor; TM, transmembrane; SPA, scintillation proximity assay; ECG, electrocardiogram.

\* Author to whom correspondence should be addressed. E-mail: Fabrizio.E.Micheli@gsk.com; Christian.A.Heidbreder@gsk.com.

<sup>§</sup> Psychiatry Centre of Excellence, GlaxoSmithKline Medicine Research Centre, Verona, Italy.

<sup>#</sup> Molecular Discovery Research, GlaxoSmithKline Medicine Research Centre, Verona, Italy.

<sup>‡</sup> Safety Assessment, GlaxoSmithKline Medicine Research Centre, Verona, Italy.

<sup>∇</sup> Neurology Centre of Excellence, GlaxoSmithKline Medicine Research Centre, Harlow, UK.

<sup>†</sup> Psychiatry Centre of Excellence, GlaxoSmithKline Medicine Research Centre, Harlow, UK.

<sup>‡</sup> Molecular Discovery Research, GlaxoSmithKline Medicine Research Centre, Harlow, UK.

<sup>||</sup> Safety Assessment, GlaxoSmithKline Medicine Research Centre, Harlow, UK.

<sup>⊗</sup> St. John's University.

<sup>⊗</sup> Current address: European Patent Office, Munich, Germany.

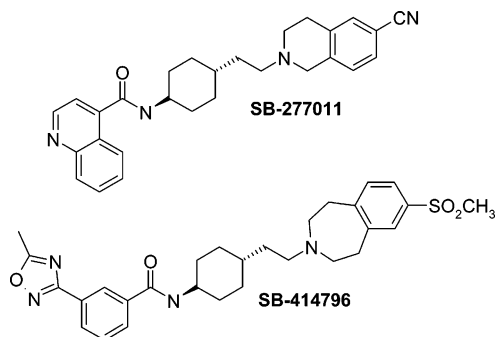


**Figure 1.** Structures of the previously reported GSK selective dopamine D<sub>3</sub> receptor antagonists.

human ether-a go-go K<sup>+</sup> channel (hERG<sup>a</sup>) affinity and the potentially related modification of the QTc<sup>51</sup> profile, was suboptimal for further development. Considerable efforts were, therefore, devoted to the identification of NCEs endowed with drug-like properties. Our main focus was directed toward the modification of our lead molecule **2**, removing the cyclohexyl ethyl linker, the sulfone and the amide moiety, which were believed to be the major cause of the poor developability profile of compound **2**. To that purpose, among the various possibilities offered by the general knowledge in the field (see ref 9 and cited references), we selected the thiothiazole group as a candidate to be introduced in the molecule, while different linkers were chosen with a focus on linear ones. Compounds of the series (Tables 1 to 3) were prepared according to the general Scheme 1 reported below. Additional information can also be found in refs 14–18, while detailed experimental parts for all of the intermediates is available as Supporting Information.

Compounds were assayed for their agonistic and antagonistic properties using a functional GTPγS assay expressing the human dopamine D<sub>3</sub> receptor. Key features of NCEs were as follows: at least 100-fold selectivity vs dopamine D<sub>2</sub> and histamine H1 receptors (functional assays), as well as a minimal requirement of 100-fold selectivity vs the hERG ion channel (dofetilide binding assay). Generic developability screens such as CYPEX bactosome P450 inhibition and rat and human in vitro clearance in liver microsomes were included early in the screening cascade.

## Results and Discussion

From the data reported in Table 1, it became evident that the newly designed thiothiazole scaffolds showed promising properties from an in vitro perspective. Compound **3** showed an almost nanomolar potency at the desired target and was endowed with a greater than 100-fold selectivity over D<sub>2</sub>, H<sub>1</sub>, and hERG. The in vitro pharmacokinetic developability screens of compound **3** revealed a cytochrome P450 profile with no inhibition on single isoforms below 10 μM and a moderate intrinsic clearance in human liver microsomes (4.7 mL/min/g). From the in silico point of view, compound **3** had a molecular weight of 525 Da, a calculated logD<sup>19</sup> of 5.9, and a polar surface area<sup>20</sup> of 73 Å<sup>2</sup>. Accordingly, **3** was tested in vivo<sup>21</sup> in rats to assess its in vivo PK profile. The results proved to be very promising, suggesting that **3** might represent an ideal template to replace **2**: the molecule was actually endowed with a moderate bioavailability in rat (27%) and had a high brain/ blood ratio (3.7). Nonetheless, being the first in a series, compound **3** had a relatively high blood clearance (Cl<sub>b</sub> 59 mL/min/kg), and its distribution volume was relatively high (7.9 L/kg). Considering the results of the in vitro profiling, the first optimization step for derivative **3**

consisted of the design of derivatives endowed with reduced clogD and lower MW (**4–7**). While no major effect was observed in terms of potency at the dopamine D<sub>3</sub> receptor, much higher hERG values were observed for compounds **4–6**. In contrast, derivative **7** showed a good in vitro profile, but its hCl<sub>i</sub> was relatively high (6.4 mL/min/g); therefore, no further activity was planned on this compound.

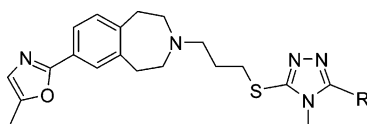
In order to address the hERG liability associated with derivatives **4–6**, the isoxazolyl moiety was chosen to replace the oxazolyl moiety to assess the role of the relative position of the heteroatoms, and derivative **8** was prepared. Also in this case (Table 2) a good in vitro profile was achieved in terms of dopamine D<sub>3</sub> vs D<sub>2</sub> potency. While B/B remained good (3.1), compound **8** showed the great advantage of a reduced distribution volume (3.4 L/kg); this profile was also associated with a lower clogD (5.2). Rat *F*% was similar to **3** (24% vs 27%), and a reduced Cl<sub>b</sub> was also observed (38 vs 59 mL/min/kg). Accordingly, compound **8** was tested in vivo and produced a significant decrease in a rat model of nicotine-triggered relapse to nicotine-seeking behavior. However, the hERG pIC<sub>50</sub> (pIC<sub>50</sub> = 6.3) still exceeded the desired selectivity profile. Functional activity at the hERG channel was also confirmed electrophysiologically<sup>22</sup> with an in vitro EC<sub>50</sub> of 0.12 μM (pIC<sub>50</sub> = 6.9), a value which produced a clear QTc prolongation in vivo when assessed in the anesthetized guinea pig.<sup>23</sup>

Despite the good potency and selectivity achieved, all the compounds reported in Table 2 that exceeded hERG dofetilide binding values of 6.5 were not progressed further along the screening cascade. The compounds with values lower than 6.5 were progressed and either failed in the developability screen or showed a suboptimal PK profile in rats. The results from the SAR exploration showed quite clearly (e.g., **20–22**) a general trend whereby increases in dopamine D<sub>3</sub> affinity were often paralleled by increases in potency at the hERG ion channel, thus suggesting common interacting features for the thiothiazole benzazepine template both at the dopamine D<sub>3</sub> receptor and at the hERG ion channel. Receptor modeling studies were then performed to identify a rational way forward in the exploration of this scaffold.

## Molecular Modeling Studies

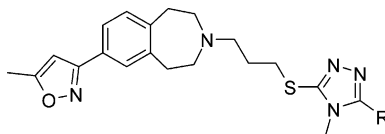
Over the last 15 years, receptor modeling and docking has become well established in the field of GPCR drug design, and more recently several computational techniques have also been developed to address hERG liability.<sup>24</sup> In the work described here a combination of docking experiments and ligand-based in silico models were used to optimize the series' properties for both the D<sub>3</sub> receptor and the hERG channel. The docking studies in particular were able to establish a molecular level understanding of the ligand–receptor/channel interactions.

Recent site-directed mutagenesis work described by Mitcheson et al.<sup>25</sup> showed that the residues Tyr652 and Phe656 on the S6 helices are the most important ones for binding a variety of ligands. They form two concentric rings of aromatic residues which line the pore cavity immediately below the ion filter. Thr623 and Val625 in the pore turn region are also important, especially for sulfonamide ligands such as MK-499.<sup>25</sup> There is still some uncertainty as to whether hERG blockers bind in the open or closed form of the channel, although most evidence would favor the open state.<sup>26</sup> Recent publications have described docking studies in both closed<sup>25</sup> and open<sup>27</sup> state models although the latter required the extensive inclusion of explicit water. In the current study, models were constructed of both the open and closed forms. Following some preliminary studies,

**Table 1.** Functional Activity at the Human Dopamine D<sub>3</sub> Receptor and Selectivity for 5-Oxazolyl Derivatives

entry	R	hD <sub>3</sub> -GTPγS fpK <sub>i</sub> <sup>b</sup>	hD <sub>2</sub> -GTPγS fpK <sub>i</sub> <sup>b</sup>	hH <sub>1</sub> -FLIPR <sup>c</sup> pK <sub>b</sub>	hERG pIC <sub>50</sub>	PSA, Å	cLogD
1	not applicable	8.4	6.4	6.2	5.7	69	3.8
2	not applicable	9.2	6.1	NT	5.6	105	2.9
3	2-methyl-5-quinolinyl	8.7	< 6.1	6.3	6.1	73	5.9
4	2-thienyl	8.5	6.6	6.4	6.5	60	5.2
5	2-indolyl	8.9	6.0	5.7	7.3	76	5.1
6	5-indolyl	8.8	6.2	6.2	7.4	76	5.5
7	N-methyl-2-pyrrolyl	8.8	5.9	6.0	6.3	65	4.2

<sup>a</sup> SEM for D<sub>3</sub> GTPγS, H1 FLIPR and hERG data sets is ±0.1 and for the D<sub>2</sub> GTPγS data is ±0.2. <sup>b</sup> fpK<sub>i</sub> = functional pK<sub>i</sub> obtained from the GTPγS functional assay. <sup>c</sup> FLIPR = fluorescent imaging plate reader.

**Table 2.** Functional Activity at the Human Dopamine D<sub>3</sub> Receptor and Selectivity for 5-Isoxazolyl Derivatives

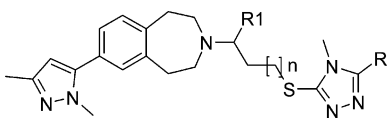
entry	R	hD <sub>3</sub> -GTPγS fpK <sub>i</sub> <sup>b</sup>	hD <sub>2</sub> -GTPγS fpK <sub>i</sub> <sup>b</sup>	hH <sub>1</sub> -FLIPR <sup>c</sup> pK <sub>b</sub>	hERG pIC <sub>50</sub>	PSA, Å	cLogD
8	2-methyl-5-quinolinyl	8.7	6.0	6.2	6.3	73	5.2
9	2-methyl-6-quinolinyl	9.0	5.7	NT	NT	73	5.2
10	2,3-dimethyl-6-quinoxaliny	8.2	5.2	NT	6.5	86	4.9
11	Ph	8.8	6.4	7.0	6.8	60	4.9
12	4-cyano Ph	8.4	6.0	NT	7.7	84	4.5
13	4-trifluoromethylphenyl	8.5	6.3	5.7	7.2	60	5.8
14	4-methylphenyl	8.8	6.4	6.5	7.6	60	5.3
15	2-pyridinyl	8.6	<5.8	6.7	6.6	73	3.8
16	4-pyridinyl	7.6	6.0	6.2	6.1	73	3.6
17	2-thienyl	8.9	6.6	7.1	6.9	60	4.5
18	1-methyl-pyrrol-2-yl	9.1	<6.4	7.4	6.6	65	3.5
19	2-chlorophenyl	8.6	6.5	6.9	7.2	60	5.0
20	3-chlorophenyl	8.8	6.7	7.4	7.1	60	5.7
21	4-chlorophenyl	9.2	6.4	7.2	7.6	60	5.6
22	3,4-dichlorophenyl	9.0	6.3	6.9	8.0	60	6.3
23	2-fluorophenyl	8.8	5.9	6.6	6.6	60	5.1
24	Me	7.4	<5.9	6.1	6.1	60	2.7
25	CF <sub>3</sub>	8.0	6.8	6.9	6.5	60	3.7
26	i-Pr	8.0	6.2	7.7	5.9	60	3.5
27	t-Bu	8.3	6.8	6.5	6.4	60	3.9
28	cyclopentyl	8.7	6.6	7.1	6.1	60	4.2
29	4-methyl-cyclohexyl	8.9	6.9	6.7	6.9	60	5.2
30	tetrahydropyran-4-yl	8.9	5.9	5.8	5.4	69	2.8
31	2-methoxyphenyl	8.5	7.1	6.7	7.4	69	4.6
32	3-methoxyphenyl	9.1	8.1	6.9	NT	69	5.0
33	4-methoxyphenyl	9.4	6.7	NT	7.4	69	5.0
34	6-methoxy-3-pyridinyl	8.6	5.9	6.60	6.8	82	4.6

<sup>a</sup> SEM for D<sub>3</sub> GTPγS, H1 FLIPR and hERG data sets is ±0.1 and for the D<sub>2</sub> GTPγS data is ±0.2. <sup>b</sup> fpK<sub>i</sub> = functional pK<sub>i</sub> obtained from the GTPγS functional assay. <sup>c</sup> FLIPR = fluorescent imaging plate reader.

however, most of the docking of the receptor antagonists was performed in the closed form of the channel, as only in this state could they interact with several of the key aromatic residues simultaneously. In addition to these docking studies, other parameters were monitored in the design phase, in particular lipophilicity and basicity.

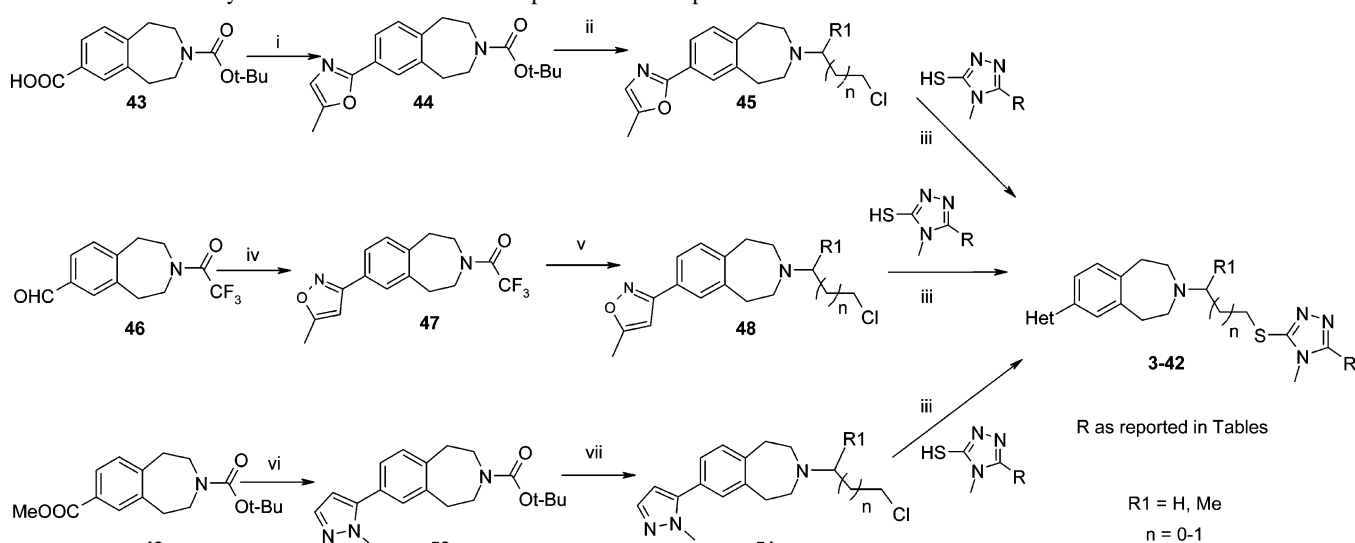
The ligands were docked manually in the hERG cavity described above, with full conformational flexibility of both the ligand and protein taken into consideration. Only low energy states of the former were allowed while the protein side chain rotamer angles were set within the limits defined by the Karplus rotamer library.<sup>28</sup> Multiple starting poses were set up which were then fully minimized. The results for compound **10** are discussed below.

Although the ligand could be docked in a linear conformation, this was only possible immediately below the ion gate, where very few interactions with the aromatic residues above were found. An alternative pose with the ligand oriented along the channel axis led to an unlikely result where one end of the ligand extended below the bottom of the helical bundle. By contrast most of the resulting poses had compound **10** in a “U-shaped” orientation as seen in Figure 2A. This is undoubtedly due to an induced fit of the ligand to the aromatic cavity. Thus, not only does the compound exhibit good interactions with all four of the Phe656 residues as well as two of the Tyr652s but the intramolecular  $\pi$ -stacking of the ligand is also entropically favored. From Figure 2A it can be seen that the protonated

**Table 3.** Functional Activity at the Human Dopamine D<sub>3</sub> Receptor and Selectivity for 5-Pyrazolyl Derivatives


entry	R	R1	n	hD <sub>3</sub> -GTPγS fpK <sub>i</sub> <sup>b</sup>	hD <sub>2</sub> -GTPγS fpK <sub>i</sub> <sup>b</sup>	hH <sub>1</sub> -FLIPR <sup>c</sup> pK <sub>b</sub>	hERG pIC <sub>50</sub>	PSA, Å	cLogD
35	2-methyl-5-quinolinyl	H	1	8.8	6.5	6.1	5.7	65	5.3
36	3,4-difluorophenyl	H	1	8.8	<6.2	5.7	6.6	52	6.0
37	4-trifluoromethylphenyl	H	1	8.1	6.3	6.3	7.5	52	5.4
38	4-methyl-1,3-oxazol-5-yl	H	1	7.9	<6.1	5.9	5.6	78	3.4
39	2-methyl-5-quinolinyl	H	0	7.8	<6.2	<5.6	5.7	65	5.8
40	5-methyl-2-pyrazinyl	H	0	8.3	<6.2	<5.6	5.7	78	4.2
41	3,4-difluorophenyl	H	0	8.7	<6.2	<5.6	6.3	52	5.8
42	2-methyl-5-quinolinyl	Me	1	8.8	<6.3	5.9	5.9	65	5.6

<sup>a</sup> SEM for D<sub>3</sub> GTPγS, H<sub>1</sub> FLIPR and hERG data sets is ±0.1 and for the D<sub>2</sub> GTPγS data is ±0.2. <sup>b</sup> fpK<sub>i</sub> = functional pK<sub>i</sub> obtained from the GTPγS functional assay. <sup>c</sup> FLIPR = fluorescent imaging plate reader.

**Scheme 1.** General Synthetic Procedures for the Preparation of Compounds 3–42<sup>a</sup>

<sup>a</sup> i: (1) C<sub>3</sub>H<sub>3</sub>NH<sub>2</sub>, *N*-(3-dimethylaminopropyl)-*N*-ethylcarbodiimide (EDC), HOBT, CH<sub>2</sub>Cl<sub>2</sub>, RT, overnight; (2) refluxing AcOH., cat. Hg(OAc)<sub>2</sub>, 2 h; ii: (1) TFA; CH<sub>2</sub>Cl<sub>2</sub>, RT, 2 h; (2): Br(CH<sub>2</sub>)<sub>3</sub>Cl or Br(CH<sub>2</sub>)<sub>2</sub>Cl, or Br(CH<sub>2</sub>)<sub>4</sub>Cl, TEA, refluxing THF, 2 h; iii: DMF, cat. NaI, K<sub>2</sub>CO<sub>3</sub>, 60 °C, 24 h; iv: (1) NH<sub>2</sub>OH·HCl/Py, RT, 3 h; (2) *N*-chlorosuccinimide (NCS), DMF, 40 °C, 1.5 h; (3) C<sub>3</sub>H<sub>5</sub>Cl, TEA, RT, overnight; v: (1) K<sub>2</sub>CO<sub>3</sub>, MeOH/H<sub>2</sub>O, 50 °C, 2 h; (2) Br(CH<sub>2</sub>)<sub>3</sub>Cl or Br(CH<sub>2</sub>)<sub>2</sub>Cl, TEA, refluxing THF, 2 h; vi: (1) C<sub>9</sub>H<sub>18</sub>N<sub>2</sub>O<sub>2</sub>; LDA; -78 °C to RT; (2) TFA; CH<sub>2</sub>Cl<sub>2</sub>, RT, 2 h; (3): Br(CH<sub>2</sub>)<sub>3</sub>Cl or Br(CH<sub>2</sub>)<sub>2</sub>Cl, TEA, refluxing THF, 2 h.

nitrogen and the triazole and quinoxaline rings all form hydrogen bonds with serines in the pore.

Compound **10** was found to adopt a similar “U-shaped” conformation” when docked into a model of the dopamine D<sub>3</sub> receptor. As clearly depicted in Figure 2B, the best putative binding mode showed a strong salt bridge between the basic benzazepine nitrogen and Asp110 on transmembrane helix 3 (TM3). This aspartate is believed to be the primary binding site for most basic compounds binding to the monoamine neurotransmitter receptors. Hydrogen bond interactions were observed between the phenylisoxazole moiety and Ser192 (TM5) and between the quinoxaline nitrogen and Ser182 (second extracellular loop) while  $\pi$ -stacking interactions were seen for the quinoxalinyli-triazole moiety with Phe345 and His349 (TM6). The D<sub>3</sub> selectivity of these compounds can be explained by the hydrogen bond between the triazole ring and Thr368. The corresponding residue in the D<sub>2</sub> receptor is a phenylalanine (Phe) which would be expected to cause a severe steric clash with these ligands.

The models, in agreement with the SAR, suggest that in compound **10** the same fragments (basic nitrogen; quinoline and oxazole) necessary for potency and selectivity at the dopamine

D<sub>3</sub> receptor are also the key features which interact “negatively” with the hERG channel. To further test this hypothesis, derivatives **24–28** were prepared and a clear association between potency and lipophilicity was observed for both targets. To maintain the potency at D<sub>3</sub> it was therefore important to keep these key interactions (Figure 2B) while, at the same time, introducing new features which might reduce activity at the hERG channel.

**Medicinal Chemistry Strategies To Address hERG Liability.** A number of approaches were used to tackle this issue. Among those approaches, two will be described based on the results of the docking studies and on general knowledge about the hERG channel. In the first one, new molecules were designed to increase the hydrophilicity (Figure 3A), by replacing the heterocyclic substituents of the template on the thiotriazole end. Favorable results were achieved in terms of reduction of hERG activity while keeping relatively high potency at the dopamine D<sub>3</sub> receptor. For example, compound **30** had a very good in vitro profile with a high potency at the dopamine D<sub>3</sub> receptor (pK<sub>i</sub> = 8.9) and a 1000-fold selectivity over dopamine D<sub>2</sub> and H<sub>1</sub> receptors. This high selectivity was also observed with respect to the hERG channel. Based on this encouraging

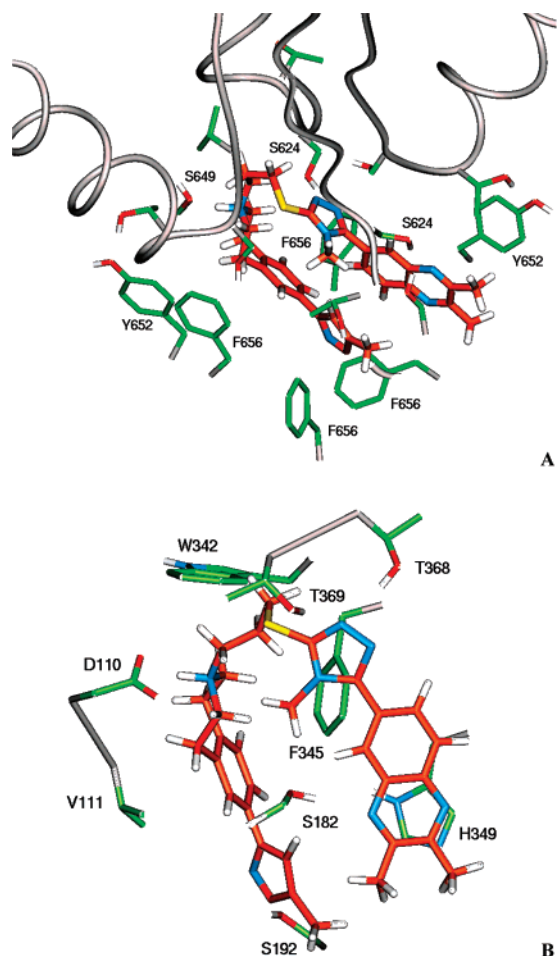


**Figure 2.** (A) Interactions of compound **10** in a “U-shaped” conformation which is energetically preferred over an extended conformation because of increased interactions with aromatic residues in the cavity. The backbone ribbon of the pore domain is included but that of the S5 and S6 helices has been removed for clarity. (B) A similar “U-shaped” conformation is found in docking to the dopamine D<sub>3</sub> receptor model. Again the backbone has been removed for clarity.

profile, a PK evaluation of **30** in the rat was performed. Bioavailability was good ( $F = 50\%$ ), with low  $V_d$  (2.4 L/kg) and low  $Cl_b$  (33 mL/min/kg). Unfortunately, brain penetration was poor ( $B/B = 0.1$ ) and so was the actual brain concentration. Considering the fact that the MW of compound **30** was 468 Da with a similar PSA to compound **8** which had a  $B/B = 3.1$  ( $PSA = 69$  vs  $73 \text{ \AA}^2$ ), the low brain concentration was probably related to the much reduced  $clogD$  (2.8 vs 5.2), unless some specific efflux mechanism was involved for this particular compound.

In the second approach, (Figure 3B), the effort was related to the reduction of  $\pi$  interaction within the hERG channel of the isoxazolyl moiety. Accordingly, specific compounds were designed to achieve a greater dihedral angle with the benzazepine moiety, also reducing PSA while maintaining MW and  $clogD$ . In house developed computational tools were used to select the appropriate bioisosteric replacements for the isoxazolyl moiety in the benzazepine class and synthetic feasibility was used to filter among the different templates. The “top scorer” of this exercise was represented by an N-methylated pyrazolyl template, and this result is clearly related to the benzazepine template here described in agreement with the specific SAR here reported.

When compound **35** (MW = 530 Da,  $clogD = 5.4$ ,  $PSA = 65 \text{ \AA}^2$ ) was prepared, it showed (Table 3) the desired in vitro

profile and achieved the appropriate selectivity over the hERG channel. Further exploration of this subseries demonstrated a SAR consistent with previously obtained results: a clear trend was once again observed between lipophilicity and hERG affinity. A slight increase in  $clogD$  with respect to **35** (e.g., **36**  $clogD = 5.5$ ) led to the same dopamine D<sub>3</sub> affinity and a slightly higher hERG value, while a marked increase in  $clogD$  (e.g., **37**  $clogD = 6.1$ ) was associated with a slight decrease in the dopamine D<sub>3</sub> affinity, but a significant increase in the hERG value ( $pIC_{50} = 7.5$  vs 5.2). Once again, an appropriately chosen hydrophilic substituent (**38**) led to a slight decrease in the dopamine D<sub>3</sub> affinity but to a marked reduction in the hERG  $pIC_{50}$ . According to the receptor and channel models, a reduction in the linker length should have provided active compounds, with a slightly reduced hERG activity. Compounds **39–41** were in agreement with the predicted potencies. Finally, the introduction of an  $\alpha$ -methyl group (**42**) should have been beneficial in terms of hERG reduction and actually an in vitro profile similar to **35** was obtained; unfortunately a very high hCli was also observed, probably due to the possible metabolic liability of the methyl group.

Compound **35** was also endowed with a P450 profile with no inhibition on single isoforms below 10  $\mu M$  and ideal hCli (1.8 mL/min/g liver) and was therefore selected for further characterization. The PK profile in rat showed a moderate  $Cl_b$  (38 mL/min/kg), acceptable  $F\%$  (15%), a low-to-moderate  $V_d$  (3.7 L/kg), and a good half-life ( $T_{1/2} = 1.7$  h); moreover, as predicted by our calculations, the B/B ratio of **35** was high (2.5).

Before submission of the compound to in vivo disease models, compound **35** was first submitted to hERG electrophysiology determination. The reported affinity was 0.43  $\mu M$  ( $pIC_{50} = 6.5$ ), leading to an almost 4-fold improvement with respect to compound **8** in accordance with the computational models. More importantly, when tested in vivo in the anesthetized guinea pig model, compound **35** showed no QTc prolongation or any cardiac liability despite a high exposure in blood ( $C_{max}$  of 34.4  $\mu g/mL$  @ 25 mg/kg).

Following these positive results, compound **35** was thoroughly characterized.

#### Further in Vitro Characterization of Compound 35.

Compound **35** displayed high selectivity over D<sub>2</sub> receptors (Table 4) and a 100-fold selectivity over a wide range of receptors and enzymes (see detailed Cerep Report in the Supporting Information). Moreover, **35** did not stimulate [<sup>35</sup>S]-GTP $\gamma$ S binding above basal levels in human recombinant dopamine D<sub>3</sub> receptors when tested alone up to a concentration of 10  $\mu M$  (Table 4). Derivative **35** behaved as a potent competitive antagonist with a  $pK_b$  derived from Schild analysis of 7.93 (slope 1.0), comparable to the value of  $pK_i$  obtained also from filtration binding data ( $D_3 = 7.99$  and  $D_2 = 5.02$ ) (Table 4). Finally, **35** was tested in a [<sup>125</sup>I]-7-OH-PIPAT competition binding assay on brain homogenates from rat nucleus accumbens and olfactory tubercles. In these saturation binding experiments, [<sup>125</sup>I]-7-OH-PIPAT bound to a single class of receptor sites with a  $pK_D$  value of  $9.34 \pm 0.11$  and a  $B_{max}$  of  $144 \pm 16 \text{ fmol mg}^{-1} \text{ protein}$  ( $n = 8$ ). Compound **35** completely displaced, in a monophasic manner, the specific [<sup>125</sup>I]-7-OH-PIPAT binding to rat membrane preparation. A  $pK_i$  value of  $8.48 \pm 0.08$  ( $n = 4$ ) was found, thus confirming a high affinity to the rat dopamine D<sub>3</sub> receptor.

**Further in Vivo Assays of Compound 35.** An in vivo study was conducted to assess the efficacy of compound **35** on the expression of nicotine-induced conditioned place preference in the rat. In the CPP paradigm, animals are given an injection of

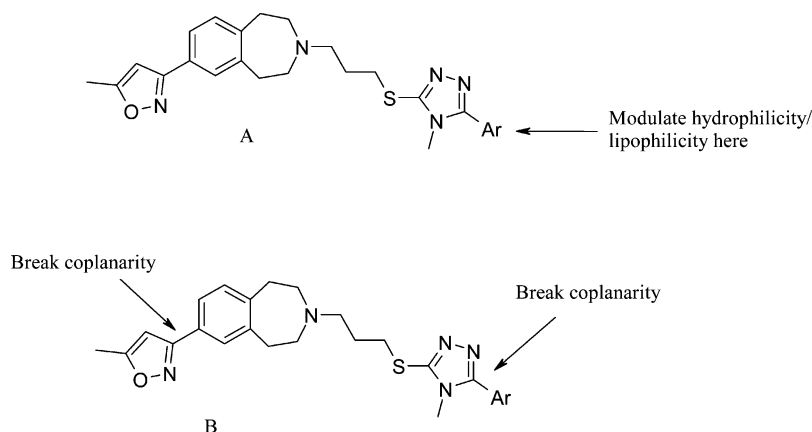


**Figure 3.** Alternative medicinal chemistry strategies to address hERG liability.

**Table 4.** Profile of Compound **35** in Human Recombinant DA D<sub>3</sub> Radioligand Binding, [<sup>35</sup>S]GTPγS Binding in Cell Membranes Expressing hDA D<sub>3</sub> Receptors, and [<sup>125</sup>I]-7-OH-PIPAT Competition Binding Assay on Brain Homogenates from Rat Brain

	pK <sub>i</sub> GTPγS		pK <sub>i</sub> filtration binding			
	hDA D <sub>3</sub>	hDA D <sub>2</sub>	hDA D <sub>3</sub>	hDA D <sub>2</sub>	pK <sub>b</sub> , hDA D <sub>3</sub>	rat native tissue, r DA D <sub>3</sub>
<b>35</b>	9.0	6.5	8.0	5.0	7.93	8.48

**Table 5.** Effect of a Single i.p. Administration of Vehicle and **35** (1, 3, 10 mg/kg) on the Expression of the Conditioned Place Preference Response to 0.4 mg/kg s.c. of (-)-Nicotine in Adult Male Sprague–Dawley Rats

treatment pairings	drug given on test day	time spent in chambers (min)	
		paired	unpaired
vehicle/vehicle	vehicle <sup>b</sup>	7.55 ± 0.22 <sup>a</sup>	7.44 ± 0.22
vehicle/nicotine	vehicle	10.07 ± 0.26 <sup>c</sup>	4.92 ± 0.26
vehicle/nicotine	<b>35</b> , 1 mg/kg	7.19 ± 0.22 <sup>d</sup>	7.80 ± 0.22
vehicle/nicotine	<b>35</b> , 3 mg/kg	6.71 ± 0.25 <sup>d</sup>	8.29 ± 0.25
vehicle/nicotine	<b>35</b> , 10 mg/kg	7.53 ± 0.22 <sup>d</sup>	7.47 ± 0.22

<sup>a</sup> Each value represents the mean number of minutes spent in each chamber ± SEM. <sup>b</sup> The vehicle was 1 mL/kg s.c. of deionized, distilled water for the pairings. The vehicle used on the test day was 1 mL/kg i.p. of 20% hydroxypropyl-β-cyclodextrin. <sup>c</sup> Significantly greater than vehicle/vehicle pairings and vehicle on the test day,  $P < 0.0001$  ANOVA and Student–Newman–Keuls test. <sup>d</sup> Significantly less than vehicle/nicotine pairings + vehicle on the test day,  $P < 0.0001$ , ANOVA and Student–Newman–Keuls test.

a drug or vehicle and confined or “paired” to a specific environment with distinct cues. This pairing of the animal with specific cues after being given vehicle or drug is repeated. Subsequently, on the test day, animals are not given any treatment (drug-free) and are allowed to freely explore the CPP apparatus to determine if they prefer an environment in which they previously received drug compared to an environment in which they previously received vehicle. If the animals approach and spend a significantly greater amount of time in the drug-paired environment, one can reasonably infer that the drug was appetitive and this appetitive value is coded in the brain and is accessible in the drug-free state.

Compound **35** (1, 3, 10 mg/kg, i.p.) significantly reduced nicotine CPP in a dose-dependent manner (one-way ANOVA:  $F_{[4,76]} = 31.7$ ;  $P < 0.0001$ ), thus confirming that it can completely reverse the incentive motivational properties of nicotine (Table 5).

A second study also assessed the efficacy of compound **35** in preventing reinstatement of nicotine-seeking behavior. In reinstatement experiments, rats are trained to self-administer drugs intravenously by pressing a lever. During a subsequent

period, the drug is no longer available, but the rats are free to try to obtain the drug (a period of “extinction training”). After extinction of responding, the ability of various events to reinstate drug-seeking can be investigated. In both human addicts and animal reinstatement models, a return to drug use can be precipitated by three distinct types of stimuli: (1) re-exposure to the drug itself, (2) exposure to environmental cues that had been previously associated with drug intake, and (3) exposure to stress. In this experiment, we showed that compound **35** (1, 3, 10 mg/kg i.p.) could prevent nicotine-triggered reinstatement of nicotine seeking behavior in a dose-dependent manner. An overall ANOVA showed that there was a significant difference between treatment groups ( $F_{[4,44]} = 5.36$ ,  $P < 0.001$ ). The Fisher’s LSD post-hoc test revealed that priming with nicotine-induced a significant increase in active lever pressing compared to priming with saline ( $P < 0.001$ ). Furthermore, compound **35** (3 and 10 mg/kg) produced a significant decrease in the number of active lever presses compared to the vehicle/nicotine group ( $P < 0.05$ ).

To exclude the possibility that these positive results were influenced by any impairment in locomotor activity or motor coordination (typical effect of mixed D<sub>3</sub>/D<sub>2</sub> receptor antagonists), **35** was also tested in the rat Rotarod. Compound **35** at a high dose of 10 mg/kg i.p. failed to affect endurance performance at any of the posttreatment times tested in the Rotarod. An ANOVA with a main factor of treatment and a repeated measurements factor of test time showed that there was no significant effect of treatment ( $F_{[2,19]} = 0.1$ ), no significant effect of test time ( $F_{[2,38]} = 2.02$ ), and no significant treatment by test time interaction ( $F_{[4,38]} = 0.35$ ).

To confirm the ability of the dopamine D<sub>3</sub> mechanism to act vs different drugs of abuse, compound **35** was also tested on the expression of cocaine-induced CPP in the rat. As previously seen with nicotine, compound **35** (1, 3, 10 mg/kg, i.p.) also significantly blocked cocaine CPP in a dose-dependent manner (one-way ANOVA:  $F_{[4,36]} = 18.09$ ;  $P < 0.0001$ ), thus confirming that it can completely reverse the incentive motivational properties of cocaine (Table 6).

We have also recently shown that **1** (10, 30 mg/kg i.p.) significantly reduced alcohol preference in alcohol Preferring

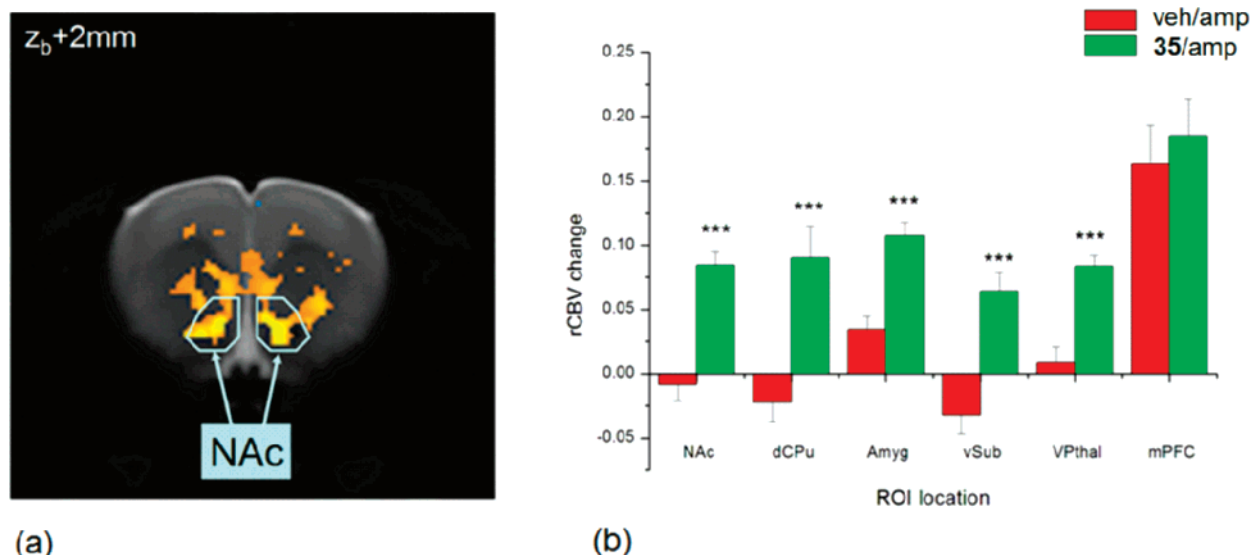


**Figure 4.** Region-specific potentiation of phMRI amphetamine (1 mg/kg i.v.) response by acute pretreatment (30 min previously) with **35** (20 mg/kg i.p.). (a) Statistical map of vehicle/amphetamine [ $n = 13$ ] vs **35**/amphetamine [ $n = 11$ ] ( $P < 0.01$ ). (b) Mean ( $\pm$ SEM) rCBV changes following amphetamine challenge for vehicle/amphetamine [ $n = 13$ ] and **35**/amphetamine [ $n = 11$ ] groups in selected ROIs, including the mPFC as a nonpotentiated control region ( $t$ -test veh/amp vs **35**/amp; \*\*\*  $P < 0.001$ ). Abbreviations: NAc = nucleus accumbens, dCPu = dorsal caudate putamen, Amyg = amygdala, vSub = ventral subiculum, VPthal = ventroposterolateral thalamic nuclei, mPFC = medial prefrontal cortex.

**Table 6.** Effect of a Single i.p. Administration of Vehicle and **35** (1, 3, 10 mg/kg) on the Expression of the Conditioned Place Preference Response to 15 mg/kg i.p. of (-)-Cocaine HCl in Adult Male Sprague–Dawley Rats

treatment pairings	drug given on test day	time spent in chambers (min)	
		paired	unpaired
vehicle/vehicle	vehicle <sup>b</sup>	7.42 $\pm$ 0.40 <sup>a</sup>	7.58 $\pm$ 0.40
vehicle/cocaine	vehicle	11.26 $\pm$ 0.48 <sup>c</sup>	3.74 $\pm$ 0.48
vehicle/cocaine	<b>35</b> , 1 mg/kg	7.58 $\pm$ 0.33 <sup>d</sup>	7.42 $\pm$ 0.33
vehicle/cocaine	<b>35</b> , 3 mg/kg	7.06 $\pm$ 0.38 <sup>d</sup>	7.94 $\pm$ 0.38
vehicle/cocaine	<b>35</b> , 10 mg/kg	8.14 $\pm$ 0.43 <sup>d</sup>	6.86 $\pm$ 0.43

<sup>a</sup> Each value represents the mean number of minutes spent in each chamber  $\pm$  SEM. <sup>b</sup> The vehicle was 1 mL/kg s.c. of deionized, distilled water for the pairings. The vehicle used on the test day was 1 mL/kg i.p. of 20% hydroxypropyl- $\beta$ -cyclodextrin. <sup>c</sup> Significantly greater than vehicle/vehicle pairings and vehicle on the test day,  $P < 0.0001$  ANOVA and Student–Newman–Keuls test. <sup>d</sup> Significantly less than vehicle/nicotine pairings + vehicle on the test day,  $P < 0.0001$ , ANOVA and Student–Newman–Keuls test.

(P) and Non-Preferring (NP) rats in a dose-dependent manner.<sup>29</sup> Similarly, **35** (1, 3, 10 mg/kg i.p.) also significantly attenuated oral operant alcohol self-administration in the C57BL/6N mouse. Our results show that compound **35** significantly decreased the number of active lever presses associated with alcohol intake (one-way ANOVA:  $F_{[3,68]} = 3.86$ ;  $P < 0.05$ ) without altering the number of inactive lever presses (one-way ANOVA:  $F_{[3,68]} = 1.19$ ;  $P = 0.32$ ).

Previous studies have shown that **1** significantly improves the learning deficit produced by the nonselective muscarinic receptor antagonist scopolamine and the anxiogenic benzodiazepine inverse agonist FG-7142 without altering the normal learning process in nonimpaired rats.<sup>30</sup> Accordingly, the effect of compound **35** (3, 10 mg/kg i.p.) on dialysate levels of ACh in the rat medial prefrontal cortex was examined. Microdialysis samples were analyzed using liquid chromatography coupled with tandem mass spectrometry (LC-MS/MS) for the detection of ACh without the use of acetylcholinesterase inhibitors.<sup>31</sup> Compound **35** (10 mg/kg i.p.) significantly increased the levels of ACh up to about 250%. These findings demonstrate that compound **35**, like other selective DA D<sub>3</sub> receptor antagonists from different chemical series,<sup>30,31</sup> increases extracellular concentrations of ACh in the rat medial prefrontal cortex and further strengthens the likelihood that selective DA D<sub>3</sub> receptor antagonists may have cognitive enhancing properties.

Finally, in analogy to what was shown in phMRI experiments in rats after acute pretreatment with **1** (i.e., potentiation of the

amplitude of the relative cerebral blood volume (rCBV) response to *d*-amphetamine in a regionally specific manner),<sup>32</sup> compound **35** (20 mg/kg i.p.) potentiated the amphetamine response in the D<sub>3</sub>-rich NAc, but also in a number of structures outside the focal distribution of the D<sub>3</sub> receptor, and associated with reinstatement of drug seeking behavior, such as the ventral subiculum region of the hippocampus, the amygdala, and striatum (Figure 4).

## Conclusions

Starting from the potent and selective dopamine D<sub>3</sub> receptor antagonist previously reported (**2**), a new series of 1,2,4-triazol-3-yl-thiopropyl-tetrahydrobenzazepines was identified. Rational design and computational tools helped us to overcome hERG-related issues and to design a number of products endowed with high affinity and selectivity for the dopamine D<sub>3</sub> receptor. In addition, selected compounds of this family series proved to have appropriate developability characteristics (P450, C<sub>1</sub>, *F*%) and good CNS penetration. In particular, compound **35** showed reduced hERG liability in vitro and no QTc prolongation in vivo. Compound **35** was shown to be a potent and selective dopamine D<sub>3</sub> receptor antagonist in vivo with no sign of locomotor liability, a typical effect produced by nonselective D<sub>3</sub>/D<sub>2</sub> receptor antagonists.

Provided that in vivo preclinical evidence can be extrapolated to human, selective DA D<sub>3</sub> receptor antagonists belonging to this new chemical series show the highest promise for the treatment of drug addiction, psychosis, and schizophrenia.

## Experimental Section

**Biological Test Methods. In Vitro Studies. Human Recombinant D<sub>3</sub> Radioligand Binding Assays.** Radioligand binding studies using [<sup>3</sup>H]-FLB-457<sup>33</sup> were performed according to the following protocol. Test compounds (10 point, half log serially diluted in 5 mM HCl) were incubated with assay buffer (50 mM TRIS, 10 mM NaCl, 5 mM KCl, 1 mM MgCl<sub>2</sub>, 2 mM CaCl<sub>2</sub>, pH 7.4), 0.2 nM [<sup>3</sup>H]-FLB-457, and CHO cell membranes containing either hD<sub>3</sub> or rD<sub>3</sub> cloned receptors for 45 min at 37 °C. Total binding was defined using 5 mM HCl, and nonspecific binding was defined using 10 μM haloperidol. The reaction was terminated by rapid filtration through GF/B filterplates presoaked in double distilled H<sub>2</sub>O, followed by 3 × 1 mL washes with ice cold 50 mM TRIS preset buffer (pH 7.7). Bound radioactivity was determined by scintillation spectrometry.

**[<sup>35</sup>S] GTPγS Functional Binding Assay in Cell Membranes Expressing hD<sub>3</sub> Receptors.** In vitro functional studies were performed according to the following [<sup>35</sup>S]-GTPγS protocol. Test compounds (10 point, half log serially diluted in assay buffer) were incubated with 10 μM GDP and CHO cell membranes containing either hD<sub>2</sub> or hD<sub>3</sub> cloned receptors for 30 min at 30 °C. 100 pM [<sup>35</sup>S]-GTPγS was added before a second incubation for 30 min at 30 °C. Basal binding was defined using assay buffer, and nonspecific binding was defined using 20 μM unlabeled GTPγS. The reaction was terminated by rapid filtration through GF/B filterplates presoaked in ddH<sub>2</sub>O, followed by 3 × 1 mL washes with ice cold 20 mM HEPES, 10 mM MgCl<sub>2</sub> buffer (pH 7.4). Bound radioactivity was determined by scintillation spectrometry.

**[<sup>125</sup>I]-7-OH-PIPAT Competition Binding Assay on Brain Homogenates from Rat Brain.** Homogenates from frozen nucleus accumbens and olfactory tubercles were prepared as described by Burris et al. (1994).<sup>34</sup> In saturation experiments, increasing concentrations of [<sup>125</sup>I]-7-OH-PIPAT (15 pM to 2 nM) were incubated with 12 μg/well of homogenates for 45 min at 37 °C in a final volume of 200 μL of 50 mM Tris-HCl (pH 7.0), 50 mM NaCl, 100 μM Gpp(NH)p and 0.02% BSA, i.e., conditions which inhibit [<sup>125</sup>I]-7-OH-PIPAT binding to D<sub>2</sub> and 5HT<sub>1A</sub> receptors.<sup>34</sup> Nonspecific binding was determined by the presence of 1 μM 1. In competition binding experiments, increasing concentrations of 35 (17 pM to 1 μM) were incubated as above in the presence of 0.1 nM [<sup>125</sup>I]-7-OH-PIPAT.

Reactions were stopped by filtration through GF/C 96-well filter plates presoaked in 0.3% polyethylenimine using a cell harvester. Filters were washed three times with 1 mL of ice-cold 50 mM Tris-HCl (pH 7.7), and radioactivity was counted in a microplate scintillation counter (Top Count, Perkin-Elmer).

Radioligand binding data were analyzed by nonlinear regression analysis using GraphPad Prism 4.0 (GraphPad Software, CA). Determination of  $K_D$  and  $B_{max}$  of [<sup>125</sup>I]-7-OH-PIPAT from saturation experiments was assessed by using one-site binding (hyperbola) equation. Curve fitting from competition-binding experiments was determined by using the one-site competition equation after checking with the *F* test ( $P < 0.05$ ) that the Hill slope in the four-parameter logistic equation was not statistically different from 1.0. Under this condition, IC<sub>50</sub> values were converted to  $K_i$  using the Cheng-Prusoff equation.<sup>33</sup> Results are expressed as mean  $pK_i \pm$  SEM.

[<sup>125</sup>I]-7-OH-PIPAT ([<sup>125</sup>I](*R*)-*trans*-7-hydroxy-2-[*N*-propyl-*N*-(3'-iodo-2'-propenyl)amino]tetralin, 81.4 TBq/mmol) was purchased from Perkin-Elmer Life and Analytical Sciences. Haloperidol and Gpp(NH)p (guanylyl-5'-imidodiphosphate) were obtained from Sigma Chemicals.

**hERG-<sup>3</sup>H-Dofetilide Binding Assay.** hERG activity was measured using <sup>3</sup>H-dofetilide binding in a scintillation proximity assay (SPA) format. The activity was measured with a Perkin-Elmer Viewlux imager.

**H1-FLIPR Assay.** A functional response in CHO-hH1 cells was measured using cytoplasmic calcium indicator Fluo-4. The change in cell fluorescence being measured in a FLIPR ( $\lambda_{ex} = 488$  nm,  $\lambda_{em} = 540$  nm, Molecular Devices, UK).

**P450 CYPEX Assay.** Inhibition (IC<sub>50</sub>) of human CYP1A2, 2C9, 2C19, 2D6, and 3A4 was determined using Cypex Bactosomes expressing the major human P450s. A range of concentrations (0.1, 0.2, 0.4, 1, 2, 4, and 10 μM) of test compound were prepared in methanol and preincubated at 37 °C for 10 min in 50 mM potassium phosphate buffer (pH 7.4) containing recombinant human CYP450 microsomal protein (0.1 mg/mL; Cypex Limited, Dundee, UK) and probe-fluorescent substrate. The final concentration of solvent was between 3 and 4.5% of the final volume. Following preincubation, NADPH regenerating system (7.8 mg of glucose 6-phosphate, 1.7 mg of NADP and 6 units of glucose 6-phosphate dehydrogenase/mL of 2% (w/v) NaHCO<sub>3</sub>; 25 μL) was added to each well to start the reaction. Production of fluorescent metabolite was then measured over a 10-min time-course using a Spectrafluor plus plate reader. The rate of metabolite production (AFU/min) was determined at each concentration of compound and converted to a percentage of the mean control rate using Magellan (Tecan software). The inhibition (IC<sub>50</sub>) of each compound was determined from the slope of the plot using Grafit v5 (Erithacus software, UK). Miconazole was added as a positive control to each plate. CYP450 isoform substrates used were ethoxyresorufin (ER; 1A2; 0.5 μM), 7-methoxy-4-trifluoromethylcoumarin-3-acetic acid (FCA; 2C9; 50 μM), 3-butyryl-7-methoxycoumarin (BMC; 2C19; 10 μM), 4-methylaminomethyl-7-methoxycoumarin (MMC; 2D6; 10 μM), diethoxyfluorescein (DEF; 3A4; 1 μM) and 7-benzyloxyquinoline (7-BQ; 3A4; 25 μM). The test was performed in three replicates.

**Intrinsic Clearance (Cl<sub>i</sub>) Assay.** Intrinsic clearance (Cl<sub>i</sub>) values were determined in rat and human liver microsomes. Test compounds (0.5 μM) were incubated at 37 °C for 30 min in 50 mM potassium phosphate buffer (pH 7.4) containing 0.5 mg microsomal protein/mL. The reaction was started by addition of cofactor (NADPH; 8 mg/mL). The final concentration of solvent was 1% of the final volume. At 0, 3, 6, 9, 15, and 30 min an aliquot (50 μL) was taken, quenched with acetonitrile containing an appropriate internal standard and analyzed by HPLC-MS/MS. The intrinsic clearance (Cl<sub>i</sub>) was determined from the first-order elimination constant by nonlinear regression using Grafit v5 (Erithacus software, UK), corrected for the volume of the incubation and assuming 52.5 mg microsomal protein/g liver for all species. Values for Cl<sub>i</sub> were expressed as mL/min/g liver. The lower limit of quantification of clearance was determined to be when <15% of the compound had been metabolized by 30 min, and this corresponded to a Cl<sub>i</sub> value of 0.5 mL/min/g liver. The upper limit was 50 mL/min/g liver.

**Patch Clamp hERG Electrophysiology Assay.** On the days of experimentation, a weighed amount of the test substance was formulated in dimethyl sulfoxide (DMSO; lot no. U10781; Sigma-Aldrich, UK) by shaking, to give a stock concentration of 10 mM of the test compound. The 10 mM stock solution was serially diluted in DMSO to give further stock solutions of 1 and 0.1 mM. Aliquots of these stock solutions were added to bath solution to achieve final perfusion concentrations of 0.1, 1, and 10 μM test compound. The corresponding vehicle concentration in all test substance perfusion solutions was 0.1% DMSO. Test substance stock formulations were freshly prepared on each day of experimentation, stored at room temperature, and protected from light.

Reference Substance: E-4031 (batch no. MLE9446; Wako Pure Chemical Industries Ltd.). Stock solutions of E-4031 (100 μM) were prepared in reverse osmosis water, aliquoted, and stored at approximately -20 °C until use. On the day of use, the 100 μM stock solution was added to bath solution to give a final perfusion concentration of 100 nM.

**Bath and Pipet Solutions:** The composition of bath solution (mM): NaCl 137; KCl 4; CaCl<sub>2</sub> 1.8; MgCl<sub>2</sub> 1.0; D-glucose 10; *N*-2-hydroxyethylpiperazine-*N'*-2-ethanesulfonic acid (HEPES) 10; pH 7.4 with 1 M NaOH. Pipet solution was prepared in batches, aliquoted, and stored frozen until the day of use. The composition of pipet solution was (mM): KCl 130; MgCl<sub>2</sub> 1.0; ethylene glycol bis(β-aminoethyl ether)-*N,N,N',N'*-tetraacetic acid (EGTA) 5; MgATP 5; HEPES 10; pH 7.2 with 1 M KOH.

**Study Design:** Cells (passage number: 48) were transferred to the recording chamber and continuously perfused (at approximately



1–2 mL/min) with bath solution at room temperature. High resistance seals (seal resistances >1.5 G $\Omega$ ) were formed between the patch electrodes (resistance range: 1.4–5.5 M $\Omega$ ) and individual cells. The membrane across the electrode tip was then ruptured, and the whole-cell patch-clamp configuration was established. Once a stable patch had been achieved, recording commenced in voltage-clamp mode, with the cell initially clamped at –80 mV. Currents were evoked by stepping the membrane potential to +20 mV and then to –50 mV (tail current). Test compound at 10, 1, and 0.1  $\mu$ M was used to produce (if any) inhibition of hERG tail current and therefore to investigate the concentration–response relationship ( $n = 3$  cells/concentration). The effect of the vehicle (0.1% DMSO) was investigated in 3 cells. The effect of 100 nM E-4031 was investigated in 2 of the vehicle-treated cells to confirm the sensitivity of the test system to an agent known to block hERG current. All perfusion solutions were applied for approximately 10 min.

**Anesthetized Guinea Pig Model for the Assessment of QT Prolongation.** Prior to the experiment, six male Hartley guinea pigs (Charles River, France) weighing between 564 and 605 g on the day of the test were anesthetized with urethane (1–1.5 g/kg IP), tracheotomized, artificially ventilated with a tidal volume of approximately 1 mL/100 g at a rate of 54 cycles/min, and surgically prepared for the experiment (i.e., insertion of catheters in appropriate blood vessels, see below, and placement of surface electrodes for lead II electrocardiogram recording). The animal's temperature was kept constant between 36.8 and 38.0  $^{\circ}$ C. Once physiological parameters were stabilized (approximately 30 min following surgery), each animal was given either the vehicle (5% w/v dextrose in aqueous 0.9 w/v sodium chloride) or test compound by the intravenous route (via the jugular vein) over 15 min/treatment.

The following parameters were recorded: arterial pressure (via the carotid artery), heart rate, electrocardiography (i.e., RR, PQ, QRS, and QT interval duration; the QT interval was corrected for heart rate changes according to Fridericia, Bazett, and Van de Water's formula). Parameters were recorded prior to dosing to establish baseline measurements and continuously during the infusion period, but data were reported every 5 min during each infusion period. In addition, blood samples (0.3 mL) were collected via the femoral artery at the end of each infusion period for toxicokinetic evaluations.

**In Vivo Studies.** All experiments were pre-reviewed and approved by a local animal care committee in accordance with the guidelines of the "Principles of Laboratory Animal Care" (NIH publication No 86-23, revised 1985) and with a Project License that was obtained according to Italian law (Art. 7, Legislative Decree no. 116, Jan 27, 1992), which acknowledges European Directive 86/609/EEC on the care and welfare of laboratory animals.

**Nicotine CPP.** Male Sprague–Dawley rats (200 g at the start of the pairings, Taconic Farms, Germantown, NY) were used in all experiments. Animals were housed two per cage, and there was no more than a 5% difference in body weight between the cagemates. Animals were kept on a 12 h lights on/12 h lights off schedule (lights on at 09.00 h). Food and water were freely available. The conditioning and testing of all animals was carried out between 11.00 and 18.00 h. All rats were naive and used only once.

An automated, two-chambered, Plexiglas CPP apparatus was used as previously described,<sup>36–38</sup> with modifications. Briefly, the two pairing chambers of the apparatus were identical in dimensions (25  $\times$  14  $\times$  36 cm) and were separated by removable Plexiglas guillotine doors. The pairing chambers were composed of distinct visual and tactile cues. The walls of one of the pairing chambers were white with cage bedding on the floor, and the walls of the second chamber consisted of alternating white and black boxes (1.2  $\times$  1.8 cm) in a chessboard pattern and a Plexiglas floor. The two pairing chambers were separated by a third, neutral connecting tunnel, with one-half of the wall white and the other half with black and white boxes.

Expression studies with compound **35** or vehicle were divided into four phases: acclimation, handling, conditioning, and testing.

The animals were not exposed to the chambers prior to the start of the pairings. During days 1–3, animals were acclimated to the animal facility. During handling (days 4–6), animals were transported to the laboratory and handled for 5 min each. During conditioning (days 7–14), animals were exposed to once-daily conditioning sessions. For each conditioning session, animals (10 rats per group) were injected with nicotine (0.6 mg/kg s.c. in a volume of 1 mL/kg) or vehicle (1 mL/kg s.c.) and then immediately confined for 30 min in an appropriate cue-specific chamber. During conditioning, nicotine was always paired with one cue-specific environment, and vehicle was paired with the other; nicotine or vehicle exposure (and appropriate environmental pairing) alternated from day to day. This was done over an 8-day period, i.e., animals were given four pairings with nicotine, and there was a 24-h separation between exposure to vehicle and nicotine. The animals in each group were randomly assigned to a 2  $\times$  2 factorial design with one factor being the pairing chamber and the other factor being the order of conditioning. In the counterbalanced procedure, the animals were randomly assigned to one of the two pairing chambers, so that half of the subjects received the drug in one compartment (white walls with bedding on the floor) and the other half in the other compartment (alternating black and white boxes with a smooth chamber floor). This procedure resulted in the animals receiving equal exposure to the two compartments and, because of random assignment, controlled for their side preference. Another group of 10 animals were paired with vehicle in both chambers of the apparatus. On the test day (day 15), animals were randomly divided into 5 groups of 10 and received compound **35** (1, 3, 10 mg/kg, i.p.) or vehicle (20% 2-hydroxypropyl- $\beta$ -cyclodextrin) in the home cage 30 min before they were placed in the apparatus and allowed free access to both chambers for 15 min. The amount of time spent in each chamber was determined using an automated timing system.

(–)-Nicotine (+)-bitartrate salt was used in all experiments (Sigma-Aldrich Corporation, St. Louis, MO) and was dissolved in sterile physiological saline and the pH adjusted to 7.4 with NaOH. The doses of nicotine were expressed as free base. 2-Hydroxypropyl- $\beta$ -cyclodextrin was purchased from Tocris-Cookson Chemical (St. Louis, MO). Data were analyzed with a one-way ANOVA with a main factor of dose. Statistical significance was set at a probability level of  $P < 0.05$ .

**Reinstatement of Nicotine-Seeking Behavior.** Male Lister Hooded rats (Charles River, Germany) were individually housed in a temperature-controlled environment with lights on from 06.00 to 18.00 h. During the experiments, water was continuously available and animals were maintained at a constant body weight of 240–260 g (85% of their ad libitum body weight).

Behavioral testing (self-administration sessions and reinstatement phase) was conducted according to the same methodology previously described and published.<sup>39</sup> Compound **35** was tested at 1, 3, and 10 mg/kg i.p. (30-min pretreatment time). The vehicle was a solution of or vehicle 20% 2-hydroxypropyl- $\beta$ -cyclodextrin. Data were analyzed by a two-way ANOVA with main factors of dose and time and repeated measurements over time. Statistical significance was set at  $P < 0.05$  for all tests.

**Rat Rotarod.** Male Lister Hooded rats (Charles River, Germany) were individually housed in a temperature-controlled environment with lights on from 06.00 to 18.00 h. During the experiments, water and food were continuously available. Rats were trained on the accelerating Rotarod (4–40 rpm over 270 s; 7750, Ugo Basile, Italy) twice daily for two consecutive days. On the test day (day 3), rats were treated with compound **35** (10 mg/kg, i.p.) ( $n = 10$  rats/group). Rats were then repeatedly tested for their endurance performance on the Rotarod 30, 60, and 120 min after treatment. Rotarod latencies were measured with a 300 s cutoff time.

**Cocaine CPP.** The cocaine CPP procedure was identical to the one described for nicotine except that for each conditioning session animals were injected with (–)-cocaine HCl (15 mg/kg i.p. in a volume of 1 mL/kg) or vehicle (1 mL/kg i.p. of deionized, distilled water). (–)-Cocaine HCl was purchased from Sigma Chemicals (St. Louis, MO).

Table 7

analytical column	Zorbax SB-C18, 4.6 × 50 mm (1.8 μm)
mobile phase	5 mM ammonium acetate + 0.1% formic acid/acetonitrile + 0.1% formic acid
gradient	97/3 → 36/64 v/v in 3.5 min → 10/90 in 3.5 min
flow rate	2.0 mL/min
detection	DAD, 210-350 nm
MS	ES+

**Alcohol Self-Administration.** Male C57BL/6N mice (Charles River, Italy), weighing approximately 27 g at the start of their training, were used in the present studies. All mice were experimentally naive, housed individually in a temperature controlled room (20–22 °C) with a 12-h light-dark cycle (06.00–18.00 light on), and had free access to tap water in their home cage.

The experiments were conducted according to the same methodology previously described and published.<sup>40</sup> The respective effects of acute treatment with compound **35** were analyzed using a two-way ANOVA with main factors of dose and session (pre vs post). The differences between individual means were assessed with the post-hoc Fisher's PLSD test. Statistical significance was set at a probability level of  $p < 0.05$  for all tests.

**Extracellular Levels of Acetylcholine in the Medial Prefrontal Cortex (mPFC).** Male Sprague–Dawley rats (Charles River, Italy) weighing 250–300 g were group housed at 21 ± 1 °C with 50% humidity on a 12/12 light–dark cycle (light-on at 6 a.m.); experiments were carried out during the light phase.

The experiments were conducted according to the same methodology previously described and published.<sup>31</sup> The effect of compound **35** on extracellular levels of ACh was analyzed by ANOVA consisting of a between-subjects factor of treatment and a repeated measurements factor of time. In addition, one-way ANOVA on the area under the curve (AUC) was performed to assess the main effect of drug treatment on ACh levels. The post-hoc Fisher's protected least significant difference pairwise comparison test was used where appropriate. Statistical significance was set at a probability level of  $p < 0.05$  for all tests.

**Pharmacological MRI.** Male Sprague–Dawley rats (250 g to 350 g; Charles-River, Como, Italy) were scanned in a Bruker Biospec 4.7T MRI scanner under 0.8% maintenance halothane anaesthesia and neuromuscular blockade; animal preparation and monitoring, and MRI setup and acquisition, were the same as published previously,<sup>32</sup> except that the time series scan comprised 16 contiguous slices of 1 mm thickness and a lower temporal resolution (80 s). The time series images were sensitized to changes in relative cerebral blood volume (rCBV) by the injection of a blood pool contrast agent (Endorem, Guerbet, France; 2.67 mL/kg) following 5 reference image frames.<sup>32,41</sup> Following 10 min equilibration, animals were administered either 20 mg/kg compound **35** ( $N = 11$ ) or vehicle saline ( $N = 13$ ) i.p., followed 30 min later by a 1 mg/kg i.v. *d*-amphetamine challenge.

The time series signal changes upon *d*-amphetamine injection were converted into rCBV changes on a pixelwise basis.<sup>41,42</sup> Following spatial coregistration of the image data, the data were smoothed with a Gaussian kernel of full-width-half-maximum equivalent to twice the in-plane pixel dimension, and the amphetamine response amplitude in each pixel was quantified by means of a general linear model analysis using the AFNI package (v2.23). Bilateral region of interest time courses corresponding to specific anatomical structures were also extracted from each subject and the rCBV changes quantified in the same way. Differences in the amphetamine response magnitude between the two groups were assessed using *t*-tests.

**Chemical Procedures. General. Experimental.** NMR spectra were obtained on Varian INOVA spectrometers (300 MHz, 400 MHz, and 500 MHz). Chemical shifts are expressed in  $\delta$  (ppm) units and peak multiplicity is expressed as follows: singlet (s), doublet (d), doublet of doublets (dd), triplet (t), multiplet (m), broad

singlet (br s), broad multiplet (br m). All mass spectrometric measurements were performed using a Micromass Platform LCZ (Waters, Manchester, UK) mass spectrometer operated in positive electrospray ionization mode. When LC/MS detection was performed, analytical conditions were used as reported in Table 7.

**General Synthetic Procedures.** For a description of the known intermediates, please refer to refs 14–18 or to the detailed experimental parts in the Supporting Information.

To a stirred solution of the appropriately decorated (oxazole, isoxazole, methylpyrazole, respectively, intermediates 44, 47, 50 reported in Scheme 1) benzazepine scaffold in THF, containing 1.1 equiv of triethylamine, was added 1-bromo-3-chloropropane (or appropriate alkylating agent) (1.1 equiv), and the solution was refluxed for 2 h. After workup and chromatographic purification, the resulting alkylating agent (respectively, 45, 48, 51 in Scheme 1) was dissolved in DMF. A catalytic amount of NaI was added and the appropriately substituted thiothiazole added together with 1.2 equiv of K<sub>2</sub>CO<sub>3</sub>. The temperature was raised to 60 °C and the suspension stirred for 24 h. The compound was purified through column chromatography (silica gel, Merck) using the appropriate mixture of cyclohexane/AcOEt. Hydrochlorides for biological testing were prepared, when necessary, dissolving the desired compounds in dichloromethane; an equimolar amount of HCl (1 M solution in Et<sub>2</sub>O) was added at room temperature, and the solvent was evaporated under reduced pressure to give the desired compounds.

**3-(3-[[4-Methyl-5-(2-methyl-5-quinolinyl)-4H-1,2,4-triazol-3-yl]thio]propyl)-7-(5-methyl-1,3-oxazol-2-yl)-2,3,4,5-tetrahydro-1H-3-benzazepine (3).** The compound was obtained as a white foam (55% yield). <sup>1</sup>H NMR (DMSO-*d*<sub>6</sub>)  $\delta$ : 2.26 (m, 2H), 2.35 (d, 3H), 2.72 (s, 3H), 3.00–3.5 (br m, 10H), 3.43 (s, 3H), 3.69 (br m, 2H), 6.96 (m, 1H), 7.35 (d, 1H), 7.55 (d, 1H), 7.72 (dd, 1H), 7.80 (m, 2H), 7.91 (t, 1H), 8.17 (d, 1H), 8.26 (br s, 1H), 10.69 (br s, 1H). MS.  $m/z = 525$  [M + H]<sup>+</sup>. Anal. (C<sub>30</sub>H<sub>32</sub>N<sub>6</sub>O<sub>2</sub>·HCl) C, H, N.

**7-(5-Methyl-1,3-oxazol-2-yl)-3-(3-[[4-methyl-5-(2-thienyl)-4H-1,2,4-triazol-3-yl]thio]propyl)-2,3,4,5-tetrahydro-1H-3-benzazepine (4).** The compound was obtained as a light brown foam (35% yield); <sup>1</sup>H NMR (DMSO-*d*<sub>6</sub>)  $\delta$ : 2.2 (m, 2H), 2.39 (s, 3H), 3.08 (m, 4H), 3.24 (m, 4H), 3.43 (m, 2H), 3.47 (m, 2H), 3.76 (s, 3H), 6.99 (m, 1H), 7.28 (dd, 1H), 7.37 (d, 1H), 7.67 (dd, 1H), 7.76 (dd, 1H), 7.8–7.83 (m, 2H), 10.83 (br s, 1H). MS.  $m/z$  466 [M + H]<sup>+</sup>. Anal. (C<sub>24</sub>H<sub>27</sub>N<sub>5</sub>O<sub>2</sub>·HCl) C, H, N.

**3-(3-[[5-(1H-Indol-2-yl)-4-methyl-4H-1,2,4-triazol-3-yl]thio]propyl)-7-(5-methyl-1,3-oxazol-2-yl)-2,3,4,5-tetrahydro-1H-3-benzazepine (5).** The compound was obtained as a light yellow foam (66% yield); <sup>1</sup>H NMR (DMSO-*d*<sub>6</sub>)  $\delta$ : 2.2 (m, 2H), 2.39 (d, 3H), 3.05–3.2 (m, 4H), 3.28 (m, 4H), 3.3–3.4 (m, 2H), 3.71 (m, 2H), 3.84 (s, 3H), 6.99 (m, 1H), 7.06 (s, 1H), 7.08 (mt, 1H), 7.22 (mt, 1H), 7.38 (d, 1H), 7.49 (d, 1H), 7.66 (d, 1H), 7.76 (dd, 1H), 7.82 (d, 1H), 10.16 (br s, 1H), 11.88 (s, 1H). MS.  $m/z$  499 [M + H]<sup>+</sup>. Anal. (C<sub>28</sub>H<sub>30</sub>N<sub>6</sub>O<sub>2</sub>·HCl) C, H, N.

**3-(3-[[5-(1H-Indol-5-yl)-4-Methyl-4H-1,2,4-triazol-3-yl]thio]propyl)-7-(5-methyl-1,3-oxazol-2-yl)-2,3,4,5-tetrahydro-1H-3-benzazepine (6).** The compound was obtained as a light brown foam (71% yield) <sup>1</sup>H NMR (DMSO-*d*<sub>6</sub>)  $\delta$ : 2.24 (m, 2H), 2.39 (d, 3H), 3.0–3.8 (m, 12H), 3.67 (s, 3H), 6.58 (m, 1H), 6.99 (m, 1H), 7.38 (d, 1H), 7.43 (dd, 1H), 7.5 (m, 1H), 7.58 (d, 1H), 7.77 (dd, 1H), 7.82 (m, 1H), 7.91 (d, 1H), 10.41 (br s, 1H), 11.44 (s, 1H). MS.  $m/z$  499 [M + H]<sup>+</sup>. Anal. (C<sub>28</sub>H<sub>30</sub>N<sub>6</sub>O<sub>2</sub>·HCl) C, H, N.

**3-(3-[[4-Methyl-5-(1-methyl-1H-pyrrol-2-yl)-4H-1,2,4-triazol-3-yl]thio]propyl)-7-(5-methyl-1,3-oxazol-2-yl)-2,3,4,5-tetrahydro-1H-3-benzazepine (7).** The compound was obtained as a brown foam (35% yield). <sup>1</sup>H NMR (DMSO-*d*<sub>6</sub>)  $\delta$ : 2.22 (m, 2H), 2.39 (d, 3H), 3.0–3.5 (m, 12H), 3.6 (s, 3H), 3.78 (s, 3H), 6.21 (dd, 1H), 6.56 (dd, 1H), 6.99 (m, 1H), 7.05 (dd, 1H), 7.38 (d, 1H), 7.76 (dd, 1H), 7.82 (d, 1H), 10.43 (br s, 1H). MS.  $m/z$  463 [M + H]<sup>+</sup>. Anal. (C<sub>25</sub>H<sub>30</sub>N<sub>6</sub>O<sub>2</sub>·HCl) C, H, N.

**7-(5-Methyl-3-isoxazolyl)-3-(3-[[4-methyl-5-(2-methyl-5-quinolinyl)-4H-1,2,4-triazol-3-yl]thio]propyl)-2,3,4,5-tetrahydro-1H-3-benzazepine (8).** The compound was obtained as a yellow foam (30% yield). <sup>1</sup>H NMR (DMSO-*d*<sub>6</sub>)  $\delta$ : 2.27 (m, 2H), 2.45 (s, 3H),

2.79 (br s, 3H), 3.09 (m, 4H), 3.3–3.8 (m, 11H), 6.74 (s, 1H), 7.36 (d, 1H), 7.66 (d, 2H), 7.73 (s, 1H), 7.89 (br m, 1H), 8 (br m, 1H), 8.25 (br m, 1H), 8.42 (br s, 1H), 10.61 (br s, 1H). MS. *m/z* 525 [M + H]<sup>+</sup>. Anal. (C<sub>30</sub>H<sub>32</sub>N<sub>6</sub>OS·HCl) C, H, N.

**7-(5-Methyl-3-isoxazolyl)-3-(3-[[4-methyl-5-(2-methyl-6-quinolinyl)-4H-1,2,4-triazol-3-yl]thio]propyl)-2,3,4,5-tetrahydro-1H-3-benzazepine (9).** The compound was obtained as a colorless oil: <sup>1</sup>H NMR (CDCl<sub>3</sub>) δ: 8.13 (3H, m), 7.92 (1H, d), 7.55 (1H, s), 7.49 (1H, d), 7.37 (1H, d), 7.16 (1H, d), 6.26 (1H, s), 3.69 (3H, s), 3.40 (2H, t), 2.97 (4H, m), 2.79 (3H, s), 2.68 (6H, m), 2.47 (3H, s), 2.06 (2H, m) MS *m/z* 525 [M + H]<sup>+</sup>. Anal. (C<sub>30</sub>H<sub>32</sub>N<sub>6</sub>OS·HCl) C, H, N.

**3-(3-[[5-(2,3-Dimethyl-6-quinolinyl)-4-methyl-4H-1,2,4-triazol-3-yl]thio]propyl)-7-(5-methyl-3-isoxazolyl)-2,3,4,5-tetrahydro-1H-3-benzazepine (10).** The compound was obtained as a light yellow foam: <sup>1</sup>H NMR (CDCl<sub>3</sub>) δ: 8.19 (1H, s), 8.11 (2H, s), 7.55 (1H, s), 7.50 (1H, d), 7.16 (1H, d), 6.26 (1H, s), 3.74 (3H, s), 3.41 (2H, t), 2.96 (4H, m), 2.78 (3H, s), 2.77 (3H, s), 2.66 (6H, m), 2.47 (3H, s), 2.06 (2H, m) MS *m/z* 540 [M + H]<sup>+</sup>. Anal. (C<sub>30</sub>H<sub>33</sub>N<sub>7</sub>OS·HCl) C, H, N.

**7-(5-Methyl-3-isoxazolyl)-3-{3-[[4-methyl-5-phenyl-4H-1,2,4-triazol-3-yl]thio]propyl}-2,3,4,5-tetrahydro-1H-3-benzazepine (11).** The compound was obtained as an off-white foam (70% yield). <sup>1</sup>H NMR (DMSO-*d*<sub>6</sub>) δ: 2.23 (m, 2H), 2.47 (s, 3H), 3.10 (m, 4H), 3.29 (t, 2H), 3.3 (m, 2H), 3.4 (m, 2H), 3.64 (s, 3H), 3.72 (br s, 2H), 6.75 (s, 1H), 7.37 (d, 1H), 7.58 (m, 3H), 7.68 (dd, 1H), 7.73–7.75 (m, 3H), 10.55 (bs, 1H). MS. *m/z* 460 [M + H]<sup>+</sup>. Anal. (C<sub>28</sub>H<sub>29</sub>N<sub>5</sub>OS·HCl) C, H, N.

**4-[4-Methyl-5-({3-[7-(5-methyl-3-isoxazolyl)-1,2,4,5-tetrahydro-3H-3-benzazepin-3-yl]propyl}thio)-4H-1,2,4-triazol-3-yl]-benzoxazole (12).** The compound was obtained as a colorless foam: <sup>1</sup>H NMR (CDCl<sub>3</sub>) δ: 7.81 (4H, s), 7.54 (1H, s), 7.49 (1H, d), 7.15 (1H, d), 6.26 (1H, s), 3.64 (3H, s), 3.41 (2H, t), 2.95 (4H, m), 2.65 (6H, m), 2.47 (3H, s), 2.05 (2H, m). MS. *m/z* 485 [M + H]<sup>+</sup>. Anal. (C<sub>27</sub>H<sub>28</sub>N<sub>6</sub>OS·HCl) C, H, N.

**7-(5-Methyl-3-isoxazolyl)-3-{3-[[4-methyl-5-[4-(trifluoromethyl)phenyl]-4H-1,2,4-triazol-3-yl]thio]propyl}-2,3,4,5-tetrahydro-1H-3-benzazepine (13).** The compound was obtained as a colorless solid (50% yield). <sup>1</sup>H NMR (CD<sub>3</sub>OD) δ: 2.37 (m, 2H), 2.5 (d, 3H), 3.1–3.3 (m, 4H), 3.4–3.5 (m, 2H), 3.39 (t, 2H), 3.47 (t, 2H), 3.76 (s, 3H), 3.87 (m, 2H), 6.58 (m, 1H), 7.39 (d, 1H), 7.7 (dd, 1H), 7.73 (d, 1H), 7.96 (m, 4H). MS. *m/z* 528 [M + H]<sup>+</sup>. Anal. (C<sub>27</sub>H<sub>28</sub>F<sub>3</sub>N<sub>5</sub>OS·HCl) C, H, N.

**7-(5-Methyl-3-isoxazolyl)-3-(3-[[4-methyl-5-(4-methylphenyl)-4H-1,2,4-triazol-3-yl]thio]propyl)-2,3,4,5-tetrahydro-1H-3-benzazepine (14).** The compound was obtained as a glassy solid (70% yield). <sup>1</sup>H NMR (CD<sub>3</sub>OD) δ: 2.45 (m, 2H), 2.50 (s, 3H), 2.53 (d, 3H), 3.1–3.3 (m, 4H), 3.4–3.54 (m, 6H), 3.82 (s, 3H), 3.8–3.9 (br m, 2H), 6.58 (m, 1H), 7.38 (d, 1H), 7.57 (d, 2H), 7.69 (dd, 1H), 7.75 (m, 3H). MS. *m/z* 474 [M + H]<sup>+</sup>. Anal. (C<sub>27</sub>H<sub>31</sub>N<sub>5</sub>OS·HCl) C, H, N.

**7-(5-Methyl-3-isoxazolyl)-3-(3-[[4-methyl-5-(2-pyridinyl)-4H-1,2,4-triazol-3-yl]thio]propyl)-2,3,4,5-tetrahydro-1H-3-benzazepine (15).** The compound was obtained as a colorless oil (50% yield). <sup>1</sup>H NMR (DMSO-*d*<sub>6</sub>) δ: 2.22 (m, 2H), 2.47 (s, 3H), 3.10 (m, 2H), 3.31 (m, 4H), 3.32–3.5 (m, 4H), 3.71 (m, 2H), 3.96 (s, 3H), 6.75 (m, 1H), 7.37 (d, 1H), 7.54 (m, 1H), 7.67 (dd, 1H), 7.73 (d, 1H), 8.02 (m, 1H), 8.14 (d, 1H), 8.74 (m, 1H), 10.4 (br s, 1H). MS. *m/z* 461 [M + H]<sup>+</sup>. Anal. (C<sub>25</sub>H<sub>28</sub>N<sub>6</sub>OS·HCl) C, H, N.

**7-(5-Methyl-3-isoxazolyl)-3-(3-[[4-methyl-5-(4-pyridinyl)-4H-1,2,4-triazol-3-yl]thio]propyl)-2,3,4,5-tetrahydro-1H-3-benzazepine (16).** The compound was obtained as light foam (70% yield). <sup>1</sup>H NMR (DMSO-*d*<sub>6</sub>) δ: 2.23 (m, 2H), 2.47 (s, 3H), 3.1 (m, 4H), 3.3 (m, 4H), 3.4 (m, 2H), 3.7 (m, 2H), 3.72 (s, 3H), 6.75 (m, 1H), 7.37 (d, 1H), 7.66 (dd, 1H), 7.73 (d, 1H), 7.82 (d, 2H), 8.81 (d, 2H), 10.56 (br s, 1H). MS. *m/z* 461 [M + H]<sup>+</sup>. Anal. (C<sub>25</sub>H<sub>28</sub>N<sub>6</sub>OS·HCl) C, H, N.

**7-(5-Methyl-3-isoxazolyl)-3-(3-[[4-methyl-5-(2-thienyl)-4H-1,2,4-triazol-3-yl]thio]propyl)-2,3,4,5-tetrahydro-1H-3-benzazepine (17).** The compound was obtained as an oil (73% yield). <sup>1</sup>H NMR (DMSO-*d*<sub>6</sub>) δ: 2.2 (m, 2H), 2.46 (s, 3H), 3.1 (m, 4H),

3.25 (t, 2H), 3.3 (m, 2H), 3.39 (m, 2H), 3.7 (br m, 2H), 3.76 (s, 3H), 6.75 (m, 1H), 7.28 (dd, 1H), 7.36 (d, 1H), 7.65–7.67 (m, 2H), 7.73 (d, 1H), 7.81 (dd, 1H), 10.55 (br s, 1H). MS. *m/z* 466 [M + H]<sup>+</sup>. Anal. (C<sub>24</sub>H<sub>27</sub>N<sub>5</sub>OS<sub>2</sub>·HCl) C, H, N.

**7-(5-Methyl-3-isoxazolyl)-3-(3-[[4-methyl-5-(1-methyl-1H-pyrrol-2-yl)-4H-1,2,4-triazol-3-yl]thio]propyl)-2,3,4,5-tetrahydro-1H-3-benzazepine (18).** The compound was obtained as a dark oil (83% yield). <sup>1</sup>H NMR (DMSO-*d*<sub>6</sub>) δ: 2.22 (m, 2H), 2.47 (s, 3H), 3.1 (m, 4H), 3.27 (t, 2H), 3.3 (m, 2H), 3.4 (m, 2H), 3.6 (s, 3H), 3.71 (br s, 2H), 3.77 (s, 3H), 6.21 (dd, 1H), 6.56 (dd, 1H), 6.75 (s, 1H), 7.05 (dd, 1H), 7.37 (d, 1H), 7.66 (dd, 1H), 7.73 (d, 1H), 10.57 (br s, 1H). MS. *m/z* 463 [M + H]<sup>+</sup>. Anal. (C<sub>25</sub>H<sub>30</sub>N<sub>6</sub>OS·HCl) C, H, N.

**3-(3-[[5-(2-Chlorophenyl)-4-methyl-4H-1,2,4-triazol-3-yl]thio]propyl)-7-(5-methyl-3-isoxazolyl)-2,3,4,5-tetrahydro-1H-3-benzazepine (19).** The compound was obtained as a colorless oil (40% yield). <sup>1</sup>H NMR (CD<sub>3</sub>OD) δ: 2.4 (m, 2H), 2.5 (s, 3H), 3.1–3.3 (m, 4H), 3.4–3.5 (m, 2H), 3.48 (m, 4H), 3.58 (s, 3H), 3.85 (m, 2H), 6.58 (s, 1H), 7.38 (d, 1H), 7.55–7.75 (m, 6H). MS. *m/z* 494 [M + H]<sup>+</sup>. Anal. (C<sub>26</sub>H<sub>28</sub>ClN<sub>5</sub>OS·HCl) C, H, N.

**3-(3-[[5-(3-Chlorophenyl)-4-methyl-4H-1,2,4-triazol-3-yl]thio]propyl)-7-(5-methyl-3-isoxazolyl)-2,3,4,5-tetrahydro-1H-3-benzazepine (20).** The compound was obtained as a colorless solid (78% yield). <sup>1</sup>H NMR (CD<sub>3</sub>OD) δ: 2.34 (m, 2H), 2.5 (s, 3H), 3.1–3.3 (m, 4H), 3.4–3.5 (m, 2H), 3.41 (t, 2H), 3.47 (t, 2H), 3.74 (s, 3H), 3.87 (m, 2H), 6.58 (m, 1H), 7.38 (d, 1H), 7.6–7.7 (m, 4H), 7.73 (s, 1H), 7.8 (m, 1H). MS. *m/z* 494 [M + H]<sup>+</sup>. Anal. (C<sub>26</sub>H<sub>28</sub>ClN<sub>5</sub>OS·HCl) C, H, N.

**3-(3-[[5-(4-Chlorophenyl)-4-methyl-4H-1,2,4-triazol-3-yl]thio]propyl)-7-(5-methyl-3-isoxazolyl)-2,3,4,5-tetrahydro-1H-3-benzazepine (21).** The compound was obtained as a colorless solid (48% yield). <sup>1</sup>H NMR (CD<sub>3</sub>OD) δ: 2.34 (m, 2H), 2.5 (d, 3H), 3.1–3.5 (br m, 6H), 3.38 (t, 2H), 3.46 (t, 2H), 3.72 (s, 3H), 3.9 (br m, 2H), 6.58 (m, 1H), 7.38 (d, 1H), 7.64 (m, 2H), 7.7 (dd, 1H), 7.74 (m, 3H). MS. *m/z* 494 [M + H]<sup>+</sup>. Anal. (C<sub>26</sub>H<sub>28</sub>ClN<sub>5</sub>OS·HCl) C, H, N.

**3-(3-[[5-(3,4-Dichlorophenyl)-4-methyl-4H-1,2,4-triazol-3-yl]thio]propyl)-7-(5-methyl-3-isoxazolyl)-2,3,4,5-tetrahydro-1H-3-benzazepine (22).** The compound was obtained as a colorless oil (68% yield). <sup>1</sup>H NMR (CD<sub>3</sub>OD) δ: 2.3 (m, 2H), 2.44 (s, 3H), 3.0–3.25 (m, 4H), 3.3–3.5 (m, 6H), 3.72 (s, 3H), 3.8 (m, 2H), 6.51 (s, 1H), 7.32 (d, 1H), 7.63 (dd, 1H), 7.68 (m, 2H), 7.81 (d, 1H), 7.95 (d, 1H). MS. *m/z* 528 [M + H]<sup>+</sup>. Anal. (C<sub>26</sub>H<sub>27</sub>Cl<sub>2</sub>N<sub>5</sub>OS·HCl) C, H, N.

**3-(3-[[5-(3-Fluorophenyl)-4-methyl-4H-1,2,4-triazol-3-yl]thio]propyl)-7-(5-methyl-3-isoxazolyl)-2,3,4,5-tetrahydro-1H-3-benzazepine (23).** The compound was obtained as a colorless oil (38% yield). <sup>1</sup>H NMR (CD<sub>3</sub>OD) δ: 2.38 (m, 2H), 2.5 (s, 3H), 3.1–3.3 (m, 4H), 3.4–3.5 (m, 2H), 3.44 (m, 4H), 3.77 (s, 3H), 3.86 (m, 2H), 6.58 (s, 1H), 7.38 (d, 1H), 7.47 (m, 1H), 7.6 (m, 2H), 7.65–7.75 (m, 3H). MS. *m/z* 478 [M + H]<sup>+</sup>. Anal. (C<sub>26</sub>H<sub>28</sub>FN<sub>5</sub>OS·HCl) C, H, N.

**3-{3-[[4,5-Dimethyl-4H-1,2,4-triazol-3-yl]thio]propyl}-7-(5-methyl-3-isoxazolyl)-2,3,4,5-tetrahydro-1H-3-benzazepine (24).** The compound was obtained as a colorless oil (52% yield). <sup>1</sup>H NMR (DMSO-*d*<sub>6</sub>) δ: 2.15 (m, 2H), 2.41 (s, 3H), 2.47 (s, 3H), 3.2 (t, 2H), 3.51 (s, 3H), 3.0–3.8 (br m, 10H), 6.75 (m, 1H), 7.36 (d, 1H), 7.66 (dd, 1H), 7.73 (d, 1H), 10.58 (br s, 1H). MS. *m/z* 398 [M + H]<sup>+</sup>. Anal. (C<sub>21</sub>H<sub>27</sub>N<sub>5</sub>OS·HCl) C, H, N.

**7-(5-Methyl-3-isoxazolyl)-3-(3-[[4-methyl-5-(trifluoromethyl)-4H-1,2,4-triazol-3-yl]thio]propyl)-2,3,4,5-tetrahydro-1H-3-benzazepine (25).** The compound was obtained as a colorless oil (79% yield). <sup>1</sup>H NMR (DMSO-*d*<sub>6</sub>) δ: 2.22 (m, 2H), 2.47 (s, 3H), 3.0–3.2 (m, 4H), 3.2–3.5 (m, 6H), 3.7 (m, 2H), 3.69 (s, 3H), 6.75 (m, 1H), 7.36 (d, 1H), 7.66 (dd, 1H), 7.73 (d, 1H), 10.59 (br s, 1H). MS. *m/z* 452 [M + H]<sup>+</sup>. Anal. (C<sub>21</sub>H<sub>24</sub>F<sub>3</sub>N<sub>5</sub>OS·HCl) C, H, N.

**7-(5-Methyl-3-isoxazolyl)-3-(3-[[4-methyl-5-(1-methylethyl)-4H-1,2,4-triazol-3-yl]thio]propyl)-2,3,4,5-tetrahydro-1H-3-benzazepine (26).** The compound was obtained as a colorless foam (49% yield). <sup>1</sup>H NMR (CD<sub>3</sub>OD) δ: 1.47 (m, 6H), 2.38 (m, 2H), 2.5 (s, 3H), 3.1–3.33 (m, 4H), 3.4–3.5 (m, 2H), 3.48 (m, 1H),

3.44 (m, 4H), 3.77 (s, 3H), 3.84 (m, 2H), 6.58 (s, 1H), 7.38 (d, 1H), 7.68 (dd, 1H), 7.72 (s, 1H). MS. *m/z* 426 [M + H]<sup>+</sup>. Anal. (C<sub>23</sub>H<sub>31</sub>N<sub>5</sub>O<sub>5</sub>·HCl) C, H, N.

**3-(3-[[5-(1,1-Dimethylethyl)-4-methyl-4H-1,2,4-triazol-3-yl]-thio]propyl)-7-(5-methyl-3-isoxazolyl)-2,3,4,5-tetrahydro-1H-3-benzazepine (27).** The compound was obtained as a colorless oil (92% yield). <sup>1</sup>H NMR (DMSO-*d*<sub>6</sub>) δ: 1.44 (s, 9H), 2.22 (m, 2H), 2.52 (s, 3H), 3.25 (t, 2H), 3.71 (s, 3H), 3.0–3.9 (m, 10H), 6.8 (s, 1H), 7.42 (d, 1H), 7.72 (dd, 1H), 7.79 (d, 1H), 10.2 (br s, 1H). MS. *m/z* 440 [M + H]<sup>+</sup>. Anal. (C<sub>24</sub>H<sub>33</sub>N<sub>5</sub>O<sub>5</sub>·HCl) C, H, N.

**3-{3-[(5-cyclopentyl-4-methyl-4H-1,2,4-triazol-3-yl)thio]propyl}-7-(5-methyl-3-isoxazolyl)-2,3,4,5-tetrahydro-1H-3-benzazepine (28).** The compound was obtained as a colorless foam (52% yield). <sup>1</sup>H NMR (CD<sub>3</sub>OD) δ: 1.90 (m, 6H), 2.29 (m, 2H), 2.38 (m, 2H), 2.5 (s, 3H), 3.05–3.25 (m, 4H), 3.4–3.5 (m, 2H), 3.53 (m, 1H), 3.4 (m, 4H), 3.76 (s, 3H), 3.84 (m, 2H), 6.58 (s, 1H), 7.38 (d, 1H), 7.68 (dd, 1H), 7.72 (br s, 1H). MS. *m/z* 452 [M + H]<sup>+</sup>. Anal. (C<sub>25</sub>H<sub>33</sub>N<sub>5</sub>O<sub>5</sub>·HCl) C, H, N.

**7-(5-Methyl-3-isoxazolyl)-3-(3-{[4-methyl-5-(4-methylcyclohexyl)-4H-1,2,4-triazol-3-yl]thio}propyl)-2,3,4,5-tetrahydro-1H-3-benzazepine (29).** The compound was obtained as a colorless oil (87% yield). <sup>1</sup>H NMR (DMSO-*d*<sub>6</sub>) δ: 0.95 (d, 3H), 1.4–1.9 (m, 9H), 2.17 (m, 2H), 2.47 (s, 3H), 2.99 (m, 1H), 3.21 (t, 2H), 3.0–3.5 (m, 8H), 3.52 (s, 3H), 3.69 (br s, 2H), 6.75 (s, 1H), 7.37 (d, 1H), 7.66 (dd, 1H), 7.73 (br s, 1H), 10.44 (br s, 1H). MS. *m/z* 480 [M + H]<sup>+</sup>. Anal. (C<sub>27</sub>H<sub>37</sub>N<sub>5</sub>O<sub>5</sub>·HCl) C, H, N.

**7-(5-Methyl-3-isoxazolyl)-3-(3-{[4-methyl-5-(tetrahydro-2H-pyran-4-yl)-4H-1,2,4-triazol-3-yl]thio}propyl)-2,3,4,5-tetrahydro-1H-3-benzazepine (30).** The compound was obtained as an off-white foam (52% yield). <sup>1</sup>H NMR (CD<sub>3</sub>OD) δ: 1.87 (m, 2H), 1.93 (m, 2H), 2.03 (m, 2H), 2.44 (s, 3H), 3.0–3.7 (m, 13H), 3.55 (m, 2H), 3.71 (s, 3H), 4.05 (m, 2H), 6.52 (m, 1H), 7.32 (d, 1H), 7.62 (dd, 1H), 7.66 (br s, 1H). MS. *m/z* 468 [M + H]<sup>+</sup>. Anal. (C<sub>25</sub>H<sub>33</sub>N<sub>5</sub>O<sub>2</sub>S·HCl) C, H, N.

**7-(5-Methyl-3-isoxazolyl)-3-[3-({4-methyl-5-(2-(methyloxy)phenyl)-4H-1,2,4-triazol-3-yl}thio)propyl]-2,3,4,5-tetrahydro-1H-3-benzazepine (31).** The compound was obtained as a colorless solid (72% yield). <sup>1</sup>H NMR (CD<sub>3</sub>OD) δ: 2.41 (m, 2H), 2.0 (s, 3H), 3.1–3.3 (m, 4H), 3.4–3.5 (m, 2H), 3.47 (m, 4H), 3.6 (s, 3H), 3.85–3.95 (m, 2H), 3.95 (s, 3H), 6.58 (m, 1H), 7.24 (t, 1H), 7.32 (d, 1H), 7.38 (d, 1H), 7.7 (dd, 1H), 7.56 (dd, 1H), 7.68–7.75 (m, 3H). MS. *m/z* 490 [M + H]<sup>+</sup>. Anal. (C<sub>27</sub>H<sub>31</sub>N<sub>5</sub>O<sub>2</sub>S·HCl) C, H, N.

**7-(5-Methyl-3-isoxazolyl)-3-[3-({4-methyl-5-[3-(methyloxy)phenyl]-4H-1,2,4-triazol-3-yl}thio)propyl]-2,3,4,5-tetrahydro-1H-3-benzazepine (32).** The compound was obtained as a colorless foam (80% yield). <sup>1</sup>H NMR (CD<sub>3</sub>OD) δ: 2.35 (m, 2H), 2.5 (s, 3H), 3.1–3.3 (m, 4H), 3.4–3.5 (m, 2H), 3.37 (t, 2H), 3.47 (t, 2H), 3.73 (s, 3H), 3.9 (m, 2H), 3.9 (s, 3H), 6.58 (s, 1H), 7.18 (m, 1H), 7.27 (m, 2H), 7.38 (d, 1H), 7.53 (t, 1H), 7.7 (dd, 1H), 7.73 (s, 1H). MS. *m/z* 490 [M + H]<sup>+</sup>. Anal. (C<sub>27</sub>H<sub>31</sub>N<sub>5</sub>O<sub>2</sub>S·HCl) C, H, N.

**7-(5-Methyl-3-isoxazolyl)-3-[3-({4-methyl-5-[4-(methyloxy)phenyl]-4H-1,2,4-triazol-3-yl}thio)propyl]-2,3,4,5-tetrahydro-1H-3-benzazepine (33).** The compound was obtained as a colorless foam (69% yield). <sup>1</sup>H NMR (CD<sub>3</sub>OD) δ: 2.4 (m, 2H), 2.5 (s, 3H), 3.1–3.3 (m, 4H), 3.4–3.5 (m, 2H), 3.46 (m, 4H), 3.79 (s, 3H), 3.87 (m, 2H), 3.94 (s, 3H), 6.58 (s, 1H), 7.24 (d, 2H), 7.38 (d, 1H), 7.7 (dd, 1H), 7.71 (d, 1H), 7.75 (d, 2H). MS. *m/z* 490 [M + H]<sup>+</sup>. Anal. (C<sub>27</sub>H<sub>31</sub>N<sub>5</sub>O<sub>2</sub>S·HCl) C, H, N.

**7-(5-Methyl-3-isoxazolyl)-3-[3-({4-methyl-5-[6-(methyloxy)-3-pyridinyl]-4H-1,2,4-triazol-3-yl}thio)propyl]-2,3,4,5-tetrahydro-1H-3-benzazepine (34).** The compound was obtained as a light hazel foam (59% yield). <sup>1</sup>H NMR (DMSO-*d*<sub>6</sub>) δ: 2.2 (m, 2H), 2.44 (s, 3H), 3.0–3.7 (m, 12H), 3.61 (s, 3H), 3.92 (s, 3H), 6.72 (s, 1H), 7.02 (d, 1H), 7.35 (d, 1H), 7.63 (dd, 1H), 7.71 (s, 1H), 8.04 (dd, 1H), 8.52 (d, 1H), 10.47 (br s, 1H). MS. *m/z* 491 [M + H]<sup>+</sup>. Anal. (C<sub>26</sub>H<sub>30</sub>N<sub>6</sub>O<sub>2</sub>S·HCl) C, H, N.

**7-(1,3-Dimethyl-1H-pyrazol-5-yl)-3-(3-{[4-methyl-5-(2-methyl-5-quinolinyl)-4H-1,2,4-triazol-3-yl]thio}propyl)-2,3,4,5-tetrahydro-1H-3-benzazepine (35).** The compound was obtained as a yellowish oil (45% yield). <sup>1</sup>H NMR (DMSO-*d*<sub>6</sub>) δ: 2.11 (s, 3H), 2.24 (m, 2H), 2.67 (s, 3H), 3.03 (m, 4H), 3.2–3.4 (m, 6H), 3.40

(s, 3H), 3.65–3.75 (m, 2H), 3.7 (s, 3H), 6.09 (s, 1H), 7.29 (m, s, 3H), 7.33 (br s, 1H), 7.48 (d, 1H), 7.74 (d, 1H), 7.86 (t, 1H), 8.12 (d, 1H), 8.18 (d, 1H), 10.6 (br s, 1H). MS. *m/z* 538 [M + H]<sup>+</sup>. Anal. (C<sub>31</sub>H<sub>35</sub>N<sub>7</sub>S·HCl) C, H, N.

**3-(3-[[5-(3,4-Difluorophenyl)-4-methyl-4H-1,2,4-triazol-3-yl]-thio]propyl)-7-(1,3-dimethyl-1H-pyrazol-5-yl)-2,3,4,5-tetrahydro-1H-3-benzazepine (36).** The compound was obtained as a colorless oil (55% yield). <sup>1</sup>H NMR (DMSO-*d*<sub>6</sub>) δ: 10.60 (bs, 1H), 7.85 (dt, 1H), 7.70–7.76 (m, 2H), 7.35 (m, 3H), 6.15 (s, 1H), 3.76 (s, 3H), 3.71 (bm, 2H), 3.65 (s, 3H), 3.40–3.20 (m, 6H), 3.09 (bm, 4H), 2.23 (m, 2H), 2.17 (s, 3H). MS. *m/z* 541 [M + H]<sup>+</sup>. Anal. (C<sub>28</sub>H<sub>31</sub>F<sub>3</sub>N<sub>6</sub>S·HCl) C, H, N.

**7-(1,3-Dimethyl-1H-pyrazol-5-yl)-3-[3-({4-methyl-5-[4-(trifluoromethyl)phenyl]-4H-1,2,4-triazol-3-yl]thio)propyl]-2,3,4,5-tetrahydro-1H-3-benzazepine (37).** The compound was obtained as a colorless foam (59% yield). <sup>1</sup>H NMR (DMSO-*d*<sub>6</sub>) δ: 10.48 (bs, 1H), 8.00 (m, 4H), 7.30 (m, 3H), 6.2 (s, 1H), 3.76–3.68 (2s, 6H), 3.70 (bm, 2H), 3.50–3.20, 3.10 (bm, 10H), 2.24 (quint., 2H), 2.17 (s, 3H). MS. *m/z* 509 [M + H]<sup>+</sup>. Anal. (C<sub>27</sub>H<sub>30</sub>F<sub>2</sub>N<sub>6</sub>S·HCl) C, H, N.

**7-(1,3-Dimethyl-1H-pyrazol-5-yl)-3-(3-{[4-methyl-5-(4-methyl-1,3-oxazol-5-yl)-4H-1,2,4-triazol-3-yl]thio}propyl)-2,3,4,5-tetrahydro-1H-3-benzazepine (38).** The compound was obtained as a light yellow oil (78% yield). <sup>1</sup>H NMR (DMSO-*d*<sub>6</sub>) δ: 10.25 (bs, 1H), 8.59 (s, 1H), 7.35 (m, 3H), 6.15 (s, 1H), 3.76 (s, 3H), 3.71 (s, 3H), 3.80–3.70 (bm, 2H), 3.40–3.20 (m, 6H), 3.09 (bm, 4H), 2.40 (s, 3H), 2.21 (m, 2H), 2.17 (s, 3H). MS. *m/z* 478 [M + H]<sup>+</sup>. Anal. (C<sub>25</sub>H<sub>31</sub>N<sub>7</sub>O<sub>5</sub>·HCl) C, H, N.

**7-(1,3-Dimethyl-1H-pyrazol-5-yl)-3-(2-{{4-methyl-5-(2-methyl-5-quinolinyl)-4H-1,2,4-triazol-3-yl}thio}ethyl)-2,3,4,5-tetrahydro-1H-3-benzazepine (39).** The compound was obtained as a yellowish foam (69% yield). <sup>1</sup>H NMR (DMSO-*d*<sub>6</sub>) δ: 10.82 (bs, 1H), 8.26 (d, 1H), 8.19 (d, 1H), 7.92 (t, 1H), 7.80 (d, 1H), 7.56 (d, 1H), 7.37 (m, 3H), 6.16 (m, 1H), 3.90–3.80 (bm, 2H), 3.77 (s, 3H), 3.70 (m, 2H), 3.65 (m, 2H), 3.46 (s, 3H), 3.50–3.10 (bm, 6H), 2.74 (s, 3H), 2.17 (s, 3H). MS. *m/z* 524 [M + H]<sup>+</sup>. Anal. (C<sub>30</sub>H<sub>33</sub>N<sub>7</sub>S·HCl) C, H, N.

**7-(1,3-Dimethyl-1H-pyrazol-5-yl)-3-(2-{{4-methyl-5-(5-methyl-2-pyrazinyl)-4H-1,2,4-triazol-3-yl}thio}ethyl)-2,3,4,5-tetrahydro-1H-3-benzazepine (40).** The compound was obtained as a brownish oil (69% yield). <sup>1</sup>H NMR (DMSO-*d*<sub>6</sub>) δ: 10.65 (bs, 1H), 9.18 (d, 1H), 8.71 (d, 1H), 7.35 (m, 3H), 6.15 (s, 1H), 3.91 (s, 3H), 3.80–3.70 (bm, 2H), 3.76 (s, 3H), 3.66 (m, 2H), 3.58 (m, 2H), 3.40–3.30. MS. *m/z* 475 [M + H]<sup>+</sup>. Anal. (C<sub>25</sub>H<sub>30</sub>N<sub>8</sub>S·HCl) C, H, N.

**3-(2-[[5-(3,4-Difluorophenyl)-4-methyl-4H-1,2,4-triazol-3-yl]-thio]ethyl)-7-(1,3-dimethyl-1H-pyrazol-5-yl)-2,3,4,5-tetrahydro-1H-3-benzazepine (41).** The compound was obtained as a colorless oil (85% yield). <sup>1</sup>H NMR (DMSO-*d*<sub>6</sub>) δ: 10.65 (bs, 1H), 7.85 (ddd, 1H), 7.63 (m, 1H), 7.35 (m, 3H), 6.15 (s, 1H), 3.80–3.70 (bm, 2H), 3.77 (s, 3H), 3.65 (s, 3H), 3.63 (m, 2H), 3.58 (m, 2H), 3.40–3.30 (bm, 2H), 3.15 (bm, 4H), 2.17 (s, 3H). MS. *m/z* 495 [M + H]<sup>+</sup>. Anal. (C<sub>26</sub>H<sub>28</sub>F<sub>2</sub>N<sub>6</sub>S·HCl) C, H, N.

**7-(1,3-Dimethyl-1H-pyrazol-5-yl)-3-(1-methyl-3-{{4-methyl-5-(2-methyl-5-quinolinyl)-4H-1,2,4-triazol-3-yl}thio}propyl)-2,3,4,5-tetrahydro-1H-3-benzazepine (42).** The compound was obtained as a yellowish foam (49% yield). <sup>1</sup>H NMR (DMSO-*d*<sub>6</sub>) δ: 10.58 (bs, 1H), 8.50 (bs, 1H), 8.27 (d, 1H), 8.00 (t, 1H), 7.89 (d, 1H), 7.67 (d, 1H), 7.28 (m, 3H), 6.09 (s, 2H), 3.7 (s, 3H), 3.60 (bm, 2H), 3.60–3.50 (m, 2H), 3.55 (m, 1H), 3.41 (s, 3H), 3.40 (m, 1H), 3.22 (m, 1H), 3.15–2.95 (m, 4H), 2.79 (s, 3H), 2.45 (m, 1H), 2.11 (s, 3H), 2.00 (m, 1H), 1.32 (d, 3H). MS. *m/z* 552 [M + H]<sup>+</sup>. Anal. (C<sub>32</sub>H<sub>37</sub>N<sub>7</sub>S·HCl) C, H, N.

**Computational Modeling. Construction of the hERG Models.** The closed state of the hERG channel was modeled based on its homology with the bacterial Kcsa structure from *Strep. lividans*, solved in 1998 by McKinnon et al.<sup>43</sup> Alignment of the pore region and the S6 helix is obvious from the key GYG motif (GFG in hERG) and the key hinge glycine in S6. The alignment of the S5 helices of hERG and Kcsa, however, was not obvious. This was based finally on the observation of a highly conserved glutamate at the extracellular side of S5 which is found in most potassium

channels. An NMR structure of the S5–SS1 loop peptide has been published<sup>44</sup> which suggests that this region is largely helical. This was added to the model as a helix-turn- $\beta$ -strand motif. The tetrameric ensemble was fully minimized using the CHARMM program,<sup>45</sup> with an initial 500 steps of Steepest Descent, followed by 5000 steps of ABNR, and a constant dielectric of 5. Helical H-bonding distance constraints were used to maintain the overall fold of the bundle.

An open state model was also built using the rat Kv1.2 structure as a template.<sup>46</sup> The same S5 glutamate, pore GYG, and S6 glycine residues were used to generate the alignment. Use was made of the S5–SS1 loop model constructed for the closed state structure, and the same CHARMM conditions were used for final refinement.

**Construction of the Dopamine D<sub>3</sub> Receptor Models.** The model of the dopamine D<sub>3</sub> receptor was built using our “in house” program GPCR\_Builder.<sup>47</sup> This is an automated 7TM receptor homology modeling program which incorporates a database of all known human and rodent Family A receptor sequences and a prealigned set of transmembrane domains for these. The models are based on the TM domain taken from the crystal structure of bovine rhodopsin.<sup>48</sup> A special set of optimized 3D templates are used to add the extracellular loops. An internal rotamer library is then applied to all residue side chains except those conserved residues known to be involved in an important functional role (e.g., the asparagines in TM1 and TM7, the aspartate on TM2, and the DRY motif on TM3). The program automatically generates a CHARMM script which can be used for model optimization and ligand docking. Typically, the same set of conditions as those described for the hERG models above were used during the minimization stage. A strict alignment between rhodopsin and dopamine D<sub>3</sub> gives rise to a very short loop length (two residues) between the disulfide-bonded cysteine in the second extracellular loop and the top of TM5. During the optimization, some unfolding of the extracellular side of TM5 is therefore allowed by relaxing the helical distance constraints in this region. This is in keeping with the reported SCAM results carried out by Javitch et al. on the D<sub>2</sub> receptor.<sup>49</sup>

**Manual Docking of Ligands in the Receptor and Channel Models.** The ligands used in this study were built in an extended conformation using the Spartan program.<sup>50</sup> Following initial optimization with molecular mechanics, further refinement was carried out at the semiempirical level using the AM1 Hamiltonian. Natural atomic orbital atom-centered charges were then derived with a single point calculation at the ab initio Hartree Fock level using a 3-21G\* basis set. The placement of the ligand in the protein was carried out manually with the Quanta program.<sup>45</sup> Multiple starting poses were used, ensuring each time that the ligand was always in an energetically acceptable conformation. For each pose the cavity residue side chains were adjusted, where necessary, by application of the rotamer library from Karplus and Dunbrack.<sup>28</sup> The complex was then optimized using the CHARMM program with 500 steps of SD followed by 5000 steps of ABNR. In addition to helical distance constraints on the protein, any expected ligand–protein hydrogen bonds were also constrained. Where appropriate, dihedral constraints were applied to the ligand’s planar aromatic centers. Visualization of the results was carried out using the Quanta program, from which the pictures in this paper were derived.

**Acknowledgment.** We would like to thank all the colleagues who helped in generating the data reported in this manuscript, in particular, Stefania Beato, Antonio Felici, Laurie Gordon, Phil Green, Alfredo Paio, Daniele Andreotti, Matteo Sartori, Kevin Read, Stefano Fontana, Monica Rigo, Serenella Zambon, Maria Anna Fedrigo, Alberto Ruffo, Claudia Mundi, Carla Marchioro, Silvia Davalli, and Mahmoud Hamdan.

**Note Added after ASAP Publication.** This manuscript was released ASAP on September 15, 2007. Due to an oversight, an incomplete list of authors was received by the Journal. The corrected version published ASAP on September 20, 2007.

**Supporting Information Available:** Cross-selectivity profile for compound **35** and additional chemistry information with synthetic details for the preparation of the intermediates are hereby reported. This material is available free of charge via the Internet at <http://pubs.acs.org>.

## References

- (1) Sokoloff, P.; Giros, B.; Martres, M. P.; Bouthenet, M. L.; Schwartz, J. C. Molecular cloning and characterization of a novel dopamine receptor (D<sub>3</sub>) as a target for neuroleptics. *Nature* **1990**, *347*, 146–151.
- (2) Diaz, J.; Lévesque, D.; Lammers, C. H.; Griffon, N.; Martres, M. P.; Schwartz, J. C.; Sokoloff, P. Phenotypical characterization of neurons expressing the dopamine D<sub>3</sub> receptor in the rat brain. *Neuroscience* **1995**, *65*, 731–745.
- (3) Diaz, J.; Pilon, C.; Le Foll, B.; Gros, C.; Triller, A.; Schwartz, J. C.; Sokoloff, P. Dopamine D<sub>3</sub> receptors expressed by all mesencephalic dopamine neurons. *J. Neurosci.* **2000**, *20*, 8677–8684.
- (4) Gurevich, E. V.; Joyce, J. N. Distribution of dopamine D<sub>3</sub> receptor expressing neurons in the human forebrain: comparison with D<sub>2</sub> receptor expressing neurons. *Neuropsychopharmacology* **1999**, *20*, 60–80.
- (5) Landwehrmeyer, B.; Mengod, G.; Palacios, J. M. Dopamine D<sub>3</sub> receptor mRNA and binding sites in human brain. *Brain Res. Mol. Brain Res.* **1993**, *18*, 187–192.
- (6) Suzuki, M.; Hurd, Y. L.; Sokoloff, P.; Schwartz, J. C.; Sedvall, G. D<sub>3</sub> dopamine receptor mRNA is widely expressed in the human brain. *Brain Res.* **1998**, *779*, 58–74.
- (7) Heidbreder, C. A.; Gardner, E. L.; Xi, Z.-X.; Thanos, P. K.; Mugnaini, M.; Hagan, J. J.; Ashby, C. R., Jr. The role of central dopamine D<sub>3</sub> receptors in drug addiction: a review of pharmacological evidence. *Brain Res. Rev.* **2005**, *49*, 77–105.
- (8) Joyce, J. N.; Millan, M. J. Dopamine D<sub>3</sub> receptor antagonists as therapeutic agents. *Drug Discovery Today* **2005**, *10*, 917–25.
- (9) Micheli, F.; Heidbreder, C. Selective dopamine D<sub>3</sub> receptor antagonists: A review 2001–2005. *Recent Pat. CNS Drug Discovery* **2006**, *1*, 271–288.
- (10) Newman, A. H.; Grundt, P.; Nader, M. A. Dopamine D<sub>3</sub> receptor partial agonists and antagonists as potential drug abuse therapeutic agents. *J. Med. Chem.* **2005**, *48*, 3663–79.
- (11) Heidbreder, C. A.; Andreoli, M.; Marcon, C.; Thanos, P. K.; Ashby, C. R., Jr.; Gardner, E. L. Role of dopamine D<sub>3</sub> receptors in the addictive properties of ethanol. *Drugs Today* **2004**, *40*, 355–65.
- (12) Reavill, C.; Taylor, S. G.; Wood, M. D.; Ashmeade, T.; Austin, N. E.; Avenell, K. Y.; Boyfield, I.; Branch, C. L.; Cilia, J.; Coldwell, M. C.; Hadley, M. S.; Hunter, A. J.; Jeffrey, P.; Jewitt, F.; Johnson, C. N.; Jones, D. N.; Medhurst, A. D.; Middlemiss, D. N.; Nash, D. J.; Riley, G. J.; Routledge, C.; Stemp, G.; Thewlis, K. M.; Trail, B.; Vong, A. K.; Hagan, J. J. Pharmacological actions of a novel, high-affinity, and selective human dopamine D<sub>3</sub> receptor antagonist, SB-277011-A. *J. Pharmacol. Exp. Ther.* **2000**, *294*, 1154–65.
- (13) Macdonald, G. J.; Branch, C. L.; Hadley, M. S.; Johnson, C. N.; Nash, D. J.; Smith, A. B.; Stemp, G.; Thewlis, K. M.; Vong, A. K.; Austin, N. E.; Jeffrey, P.; Winborn, K. Y.; Boyfield, I.; Hagan, J. J.; Middlemiss, D. N.; Reavill, C.; Riley, G. J.; Watson, J. M. Wood, M.; Parker, S. G.; Ashby, C. R., Jr. Design and synthesis of *trans*-3-(2-(4-((3-(3-(5-methyl-1,2,4-oxadiazolyl)-phenyl)carboxamido)cyclohexyl)ethyl)-7-methylsulfonyl-2,3,4,5-tetrahydro-1H-3-benzazepine (SB-414796): a potent and selective dopamine D<sub>3</sub> receptor antagonist. *J. Med. Chem.* **2003**, *46*, 4952–64.
- (14) Hadley, M. S.; Lightfoot, A. P.; MacDonal, G. J.; Stemp, G. Preparation of tetrahydrobenzazepines as modulators of dopamine D<sub>3</sub> receptors useful as antipsychotic agents. WO 2002040471, 2001.
- (15) Bonanomi, G.; Damiani, F.; Gentile, G.; Hamprecht, D. W.; Micheli, F.; Tarsi, L.; Tedesco, G.; Terreni, S. Preparation of fused benzazepines having affinity for dopamine D<sub>3</sub> receptor. WO 2005118549, 2005.
- (16) Hamprecht, D.; Micheli, F.; Tarsi, L.; Tedesco, G. Preparation of 7-pyrazolylbenzazepines having affinity for D<sub>3</sub> receptor. WO 2005123717, 2005.
- (17) Bonanomi, G.; Cardullo, F.; Damiani, F.; Gentile, G.; Hamprecht, D.; Micheli, F.; Tarsi, L. Preparation of fused benzazepines having affinity for the dopamine D<sub>3</sub> receptor. WO 2006002928, 2005.
- (18) Arista, L.; Bonanomi, G.; Damiani, F.; Hamprecht, D.; Micheli, F.; Tarsi, L.; Tedesco, G. Preparation of tetrahydrobenzazepine derivatives as modulators of dopamine D<sub>3</sub> receptors. WO 2005087764, 2005.
- (19) ACD Labs suite is available from <http://www.acdlabs.com>.
- (20) Ertl, P.; Rohde, B.; Selzer, P. Fast Calculation of Molecular Polar Surface Area as a Sum of Fragment-Based Contributions and Its Application to the Prediction of Drug Transport Properties. *J. Med. Chem.* **2000**, *43*, 3714–3717.

- (21) The research complied with national legislation and with company policy on the Care and Use of Animals and with related codes of practice.
- (22) Aptuit Limited, 3 Simpson Parkway, Livingston, West Lothian, EH54 7BH, Scotland. www.apuit.uk.
- (23) CERB, Chemin de Montifault, 18800 Baugy, France. www.cerb.fr.
- (24) Jamieson, C.; Moir, E. M.; Rankovic, Z.; Wishart, G. Medicinal chemistry of hERG optimizations: Highlights and hang-ups. *J. Med. Chem.* **2006**, *49*, 5029–5046.
- (25) Mitcheson, J. S.; Chen, J.; Lin, M.; Culberson, C.; Sanguinetti, M. C. A structural basis for drug-induced long QT syndrome. *Proc. Natl. Acad. Sci. U.S.A.* **2000**, *97*, 12329–333.
- (26) Sanguinetti, M. C.; Mitcheson, J. S. Predicting drug-hERG channel interactions that cause acquired long QT syndrome. *Trends Pharmacol. Sci.* **2005**, *26*, 119–124.
- (27) Oesterberg, F.; Aqvist, J. Exploring blocker binding to a homology model of the open hERG K<sup>+</sup> channel using docking and molecular dynamics methods. *FEBS Lett.* **2005**, *579*, 2939–2944.
- (28) Dunbrack, R. L., Jr.; Karplus, M. Backbone-dependent rotamer library for proteins. Application to side-chain prediction. *J. Mol. Biol.* **1993**, *230*, 543–74.
- (29) Thanos, P. K.; Katana, J. M.; Ashby, C. R., Jr.; Michaelides, M.; Gardner, E. L.; Heidbreder, C. A.; Volkow, N. D. A novel dopamine D<sub>3</sub> receptor antagonist (SB-277011-A) attenuates ethanol consumption in ethanol preferring (P) and non-preferring (NP) rats. *Pharmacol. Biochem. Behav.* **2005**, *81*, 190–197.
- (30) Laszy, J.; Laszlovszky, I.; Gyertyán, I. Dopamine D<sub>3</sub> receptor antagonists improve the learning performance of memory-impaired rats. *Psychopharmacology* **2005**, *179*, 567–575.
- (31) Lacroix, L. P.; Ceolin, L.; Zocchi, A.; Varnier, G.; Garzotti, M.; Curcuruto, O.; Heidbreder, C. A. Selective dopamine D(3) receptor antagonists enhance cortical acetylcholine levels measured with high-performance liquid chromatography/tandem mass spectrometry without anti-cholinesterases. *J. Neurosci. Methods* **2006**, *157*, 25–31.
- (32) Schwarz, A.; Gozzi, A.; Reese, T.; Bertani, S.; Crestan, V.; Hagan, J.; Heidbreder, C.; Bifone, A. Selective dopamine D<sub>3</sub> receptor antagonist SB-277011-A potentiates phMRI response to acute amphetamine challenge in the rat brain. *Synapse* **2004**, *54*, 1–10.
- (33) Okauchi, T.; Suhara, T.; Maeda, J.; Kawabe, K.; Obayashi, S.; Suzuki, K. Effect of endogenous dopamine on endogenous dopamine on extrastriated [(11)C]FLB 457 binding measured by PET. *Synapse* **2001**, *41*, 87–95.
- (34) Burris, K. D.; Filtz, T. M.; Chumpradit, S.; Kung, M. P.; Foulon, C.; Hensler, J. G.; Kung, H. F.; Molinoff, P. B. Characterization of [125I](R)-trans-7-hydroxy-2-[N-propyl-N-(3'-iodo-2'-propenyl)amino]tetralin binding to dopamine D<sub>3</sub> receptors in rat olfactory tubercle. *J. Pharmacol. Exp. Ther.* **1994**, *268*, 935–942.
- (35) Cheng, Y.; Prusoff, W. H. Relationship between the inhibition constant (K<sub>i</sub>) and the concentration of inhibitor which causes 50 per cent inhibition (I<sub>50</sub>) of an enzymatic reaction. *Biochem. Pharmacol.* **1973**, *22*, 3099–3108.
- (36) Dewey, S. L.; Brodie, J. D.; Gerasimov, M.; Horan, B.; Gardner, E. L.; Ashby, C. R., Jr. A pharmacologic strategy for the treatment of nicotine addiction. *Synapse* **1999**, *31*, 76–86.
- (37) Horan, B.; Smith, M.; Gardner, E. L.; Lepore, M.; Ashby, C. R., Jr. (-)-Nicotine produces conditioned place preference in Lewis, but not Fischer 344 rats. *Synapse* **1997**, *26*, 93–94.
- (38) Horan, B.; Gardner, E. L.; Dewey, S. L.; Brodie, J. D.; Ashby, C. R., Jr. The selective sigma(1) receptor agonist, 1-(3,4-dimethoxyphenethyl)-4-(phenylpropyl)piperazine (SA4503), blocks the acquisition of the conditioned place preference response to (-)-nicotine in rats. *Eur. J. Pharmacol.* **2001**, *426*, R1–2.
- (39) Andreoli, M.; Tessari, M.; Pilla, M.; Valerio, E.; Hagan, J. J.; Heidbreder, C. A. Selective antagonism at dopamine D<sub>3</sub> receptors prevents nicotine-triggered relapse to nicotine-seeking behavior. *Neuropsychopharmacology* **2003**, *28*, 1272–1280.
- (40) Heidbreder, C. A.; Andreoli, M.; Marcon, C.; Gardner, E. L.; Ashby, C. R., Jr. Evidence for the role of dopamine D<sub>3</sub> receptors in oral operant ethanol reinforcement and reinstatement of ethanol seeking responding in mice. *Addict. Biol.* **2007**, *12*, 35–50.
- (41) Schwarz, A. J.; Reese, T.; Gozzi, A.; Bifone, A. Functional MRI using intravascular contrast agents: detrending of the relative cerebrovascular (rCBV) time course. *Magn. Reson. Imaging* **2003**, *21*, 1191–1200.
- (42) Schwarz, A.; Whitcher, B.; Reese, T.; Gozzi, A.; Bifone, A. In *Group-level data-driven phMRI analysis*. Proceedings of the International Society for Magnetic Resonance in Medicine, 2005, 13, 157.
- (43) Kaab, S.; Dixon, J.; Duc, J.; Ashen, D.; Nabauer, M.; Beuckelmann, D. J.; Steinbeck, G.; McKinnon, D.; Tomaselli, G. F. Molecular basis of transient outward potassium current downregulation in human heart failure: a decrease in Kv4.3 mRNA correlates with a reduction in current density. *Circulation* **1998**, *98*, 1383–1393.
- (44) Torres, A. M.; Bansal, P. S.; Sunde, M.; Clarke, C. E.; Bursill, J. A.; Smith, D. J.; Bauskin, A.; Breit, S. N.; Campbell, T. J.; Alewood, P. F.; Kuchel, P. W.; Vandenberg, J. I. Structure of the HERG K<sup>+</sup> Channel S5P Extracellular Linker: Role of an Amphipathic  $\alpha$ -Helix in C-Type Inactivation. *J. Biol. Chem.* **2003**, *278*, 42136–42148.
- (45) www.accelrys.com.
- (46) Magis, C.; Gasparini, D.; Lecoq, A.; Le Du, M. H.; Stura, E.; Charbonnier, J. B.; Mourier, G.; Boulain, J.-C.; Pardo, L.; Caruana, A.; Joly, A.; Lefranc, M.; Masella, M.; Menez, A.; Cuniasse, P. Structure-Based Secondary Structure-Independent Approach To Design Protein Ligands: Application to the Design of Kv1.2 Potassium Channel Blockers. *J. Am. Chem. Soc.* **2006**, *128*, 16190–16205.
- (47) Blaney, F. E.; Tennant, M. Computational tools and results in the construction of G protein-coupled receptor models. In *Membrane Protein Models*; Findlay, J. B. C., Ed.; Bios Scientific Publishers Ltd., Oxford, UK, 1996; pp 161–176.
- (48) Polczewski, K.; Kumasaka, T.; Hori, T.; Behnke, C. A.; Motoshima, H.; Fox, B. A.; Le Trong, I.; Teller, D. C.; Okada, T.; Stenkamp, R. E.; Yamamoto, M.; Miyano, M. 2000. Crystal structure of rhodopsin: A G protein-coupled receptor. *Science* **2000**, *289*, 739–745.
- (49) Shi, L.; Simpson, M. M.; Ballesteros, J. A.; Javitch, J. A. The First Transmembrane Segment of the Dopamine D<sub>2</sub> Receptor: Accessibility in the Binding-Site Crevice and Position in the Transmembrane Bundle. *Biochemistry* **2001**, *40*, 12339–12348.
- (50) www.wavefun.com.
- (51) An undesirable feature of some drugs is their ability to delay cardiac repolarization, an effect that can be measured as prolongation of the QT interval on the surface electrocardiogram (ECG). Because of its inverse relationship to heart rate, the QT interval is routinely transformed (normalized) by means of various formulas into a heart rate independent “corrected” value known as the QTc interval. The QTc interval is intended to represent the QT interval at a standardized heart rate of 60 bpm.

JM0705612